erance and endovascular activity of human uterine NK cells at the maternal-fetal interface. *J. Immunol.* 182: 4085–4092.
36. Kalkunte, S., C. O. Chichester, F. Gotsch, C. L. Sentman, R. Romero, and S. Sharma. 2008. Evolution of non-cytotoxic uterine natural killer cells. *Am. J. Reprod. Immunol.* 59: 425–432.
37. Murphy, S. P., N. N. Hanna, L. D. Fast, S. K. Shaw, G. Berg, J. F. Padbury, R. Romero, and S. Sharma. 2008. Evidence for participation of uterine natural killer cells in the mechanisms responsible for spontaneous preterm labor and delivery. *Am. J. Obstet. Gynecol.* 200: 308e.1–308.e9.
38. Murphy, S. P., L. D. Fast, N. N. Hanna, and S. Sharma. 2005. Uterine NK cells mediate inflammation-induced fetal demise in IL-10-null mice. *J. Immunol.* 175: 4084–4090.
39. Aris, A., F. Lambert, P. Bessette, and J. M. Moutquin. 2008. Maternal circulating interferon-γ and interleukin-6 as biomarkers of Th1/Th2 immune status throughout pregnancy. *J. Obstet. Gynaecol. Res.* 34: 7–11. PubMed
40. Piccinni, M. P. 2010. T cell tolerance towards the fetal allograft. *J. Reprod. Immunol.* 85: 71–75.

THE JOURNAL OF IMMUNOLOGY

E2A and CBP/p300 Act in Synergy To Promote Chromatin Accessibility of the Immunoglobulin κ Locus

Shuji Sakamoto, Kousho Wakae, Yuki Anzai, Kiyohito Murai, Nobuyuki Tamaki, Masaki Miyazaki, Kazuko Miyazaki, William J. Romanow, Tomokatsu Ikawa, Daisuke Kitamura, Itaru Yanagihara, Nagahiro Minato, Cornelis Murre and Yasutoshi Agata

J Immunol; Prepublished online 27 April 2012;
doi:10.4049/jimmunol.1002346
http://www.jimmunol.org/content/early/2012/04/27/jimmunol.1002346

The Journal of Immunology is published twice each month by
The American Association of Immunologists, Inc.,
9650 Rockville Pike, Bethesda, MD 20814-3994.

Print ISSN: 0022-1767 Online ISSN: 1550-6606.

ublished April 27, 2012, doi:10.4049/jimmunol.1002346

E2A and CBP/p300 Act in Synergy To Promote Chromatin Accessibility of the Immunoglobulin κ Locus

Shuji Sakamoto,*[,1,2] Kousho Wakae,[†,1] Yuki Anzai,[†,1] Kiyohito Murai,* Nobuyuki Tamaki,* Masaki Miyazaki,[‡] Kazuko Miyazaki,[‡] William J. Romanow,[‡] Tomokatsu Ikawa,[§] Daisuke Kitamura,[¶] Itaru Yanagihara,[‖] Nagahiro Minato,[†] Cornelis Murre,[‡] and Yasutoshi Agata*[,†,‡,‖,1]

V(D)J recombination of Ig and TCR genes is strictly regulated in a lineage- and stage-specific manner by the accessibility of target gene chromatin to the recombinases RAG1 and RAG2. It has been shown that enforced expression of the basic helix–loop–helix protein, E2A, together with RAG1/2 in a nonlymphoid cell line BOSC23 can induce V(D)J recombination in endogenous *Igκ* and TCR loci by increasing chromatin accessibility of target gene segments. In this study, we demonstrate that ectopically expressed E2A proteins in BOSC23 cells have the ability to bind directly to the promoter and recombination signal sequence of Vκ genes and to recruit histone acetyltransferase CBP/p300. Overexpression of CBP/p300 in conjunction with E2A results in enhancement of E2A-induced histone acetylation, germline transcription, and *Igκ* rearrangement. Conversely, knockdown of endogenous CBP/p300 expression by small interfering RNA leads to a decrease in histone acetylation, germline transcription and *Igκ* rearrangement. Furthermore, analyses using a mouse pre-B cell line revealed that endogenous E2A proteins also bind to a distinct set of Vκ genes and regulatory regions in the mouse *Igκ* locus and act to increase histone acetylation by recruiting p300, confirming the similar findings observed with BOSC23 cells. These observations indicate that E2A plays critical roles in inducing *Igκ* rearrangement by directly binding to and increasing chromatin accessibility at target gene segments. *The Journal of Immunology*, 2012, 188: 000–000.

Diverse Ag receptor repertoires of lymphocytes are generated by V(D)J recombination, which assembles variable (V), diversity (D), and joining (J) gene segments within the Ig and TCR loci during B and T cell development (1–3). V(D)J recombination is initiated by recombination activating gene products, RAG1 and RAG2, which introduce double-strand breaks between coding gene segments and flanking recombination signal sequences (RSSs). The lymphocyte-specific expression of RAG proteins ensures that rearrangement is restricted to developing B and T lymphocytes. Furthermore, V(D)J recombination is strictly regulated in a lineage- and stage-specific manner. Productive rearrangement of Ig and TCR loci occurs only in B and T lymphocytes, respectively. In developing B cells, Ig H chain (*Igh*) locus rearrangement takes place at the pro-B cell stage prior to Ig L chain (*IgL*) gene recombination, which generally occurs in the pre-B cell compartment. Between the two *IgL* genes, the *Igκ* locus rearranges prior to *Igλ* VJ joining. Moreover, within the *Igh* locus, D-J rearrangements precede V-DJ rearrangements. In several Ig and TCR loci, productive VDJ rearrangement occurs only on a single allele, named allelic exclusion.

These lineage- and stage-specific rearrangements are regulated mainly by the accessibility of target gene segments to the RAG proteins (1, 3). Accessibility is typically associated with transcription of target gene segments prior to recombination, termed germline transcription, and with histone modifications such as acetylation of histone H3 and H4 as well as lysine 4-methylated histone H3. However, it is still largely unknown which factors are involved in specific targeting of the accessibility of certain gene segments in the correct lineage and at the appropriate developmental stages.

*Horizontal Medical Research Organization, Graduate School of Medicine, Kyoto University, Kyoto 606-8501, Japan; [†]Department of Immunology and Cell Biology, Graduate School of Medicine, Kyoto University, Kyoto 606-8501, Japan; [‡]Division of Biological Sciences, University of California, San Diego, La Jolla, CA 92093; [§]Laboratory for Lymphocyte Development, RIKEN Research Center for Allergy and Immunology, Yokohama 230-0045, Japan; [¶]Division of Molecular Biology, Research Institute for Biomedical Sciences, Tokyo University of Science, Noda, Chiba 278-0022, Japan; and [‖]Department of Developmental Medicine, Research Institute, Osaka Medical Center for Maternal and Child Health, Osaka 594-1101, Japan

[1]S.S., K.W., Y. Anzai, and Y. Agata contributed equally to this work.

[2]Current address: Laboratory of Molecular Biology, Science Research Center, Kochi Medical School, Kochi, Japan.

Received for publication July 12, 2010. Accepted for publication April 3, 2012.

This work was supported by grants from the Special Coordination Funds for Promoting Science and Technology, Grants-in-Aid for Scientific Research from the Ministry of Education, Culture, Sports, Science and Technology of Japan (20590298, 20060040, 22021021, 23118515, and 23390068), the Uehara Memorial Foundation, the Takeda Science Foundation, the Sankyo Foundation of Life Science, and the Astellas Foundation for Research on Metabolic Disorders.

Address correspondence and reprint requests to Dr. Yasutoshi Agata, Graduate School of Medicine, Kyoto University, Yoshida-konoe-cho, Sakyo-ku, Kyoto 606-8501, Japan. E-mail address: yagata@imm.med.kyoto-u.ac.jp

The online version of this article contains supplemental material.

Abbreviations used in this article: ChIP, chromatin immunoprecipitation; Cκ, C region of *Igκ*; 3′Eκ, 3′ *Igκ* enhancer; GLT, germline transcription; H3K9ac, acetylated histone H3 lysine 9; H3K9/14ac, diacetylated histone H3 lysine 9 and 14; H3K14ac, acetylated histone H3 lysine 14; H3K18ac, acetylated histone H3 lysine 18; H3K23ac, acetylated histone H3 lysine 23; H3K4me2, dimethylated histone H3 lysine 4; H3K4me3, trimethylated histone H3 lysine 4; H3K9me2, dimethylated histone H3 lysine 9; HA, hemagglutinin; HAT, histone acetyltransferase; H4K5/8/12/16ac, tetra-acetylated histone H4 lysine 5, 8, 12, and 16; iEκ, intronic *Igκ* enhancer; LM-PCR, ligation-mediated PCR; miRNA, microRNA; RNAi, RNA interference; RSS, recombination signal sequence; SBE, signal broken end; siRNA, small interfering RNA.

www.jimmunol.org/cgi/doi/10.4049/jimmunol.1002346

Rearrangement of the Ag receptor loci is regulated by *cis*-acting regulatory elements including transcriptional enhancers and promoters (4). Specifically, the *Igκ* locus activation is mediated by *cis*-acting regulatory elements that include two distinct enhancers, the intronic enhancer (iEκ) present between the Jκ gene segments and the exon encoding the C region of *Igκ* (Cκ), and the 3′ enhancer (3′Eκ) present downstream of the Cκ exon (5). *Igκ* recombination is diminished upon deletion of either enhancer and completely abolished in the combined-mutant mice, suggesting a functional redundancy between iEκ and 3′Eκ (6).

Among the Ig enhancer binding proteins are members of the basic helix–loop–helix family, including E12 and E47, which are alternative splicing products of the *E2A* gene and belong to the class I helix–loop–helix proteins (also called E-proteins) together with HEB and E2-2 (7). These E-proteins bind to the E-box sites (CANNTG) present in many regulatory elements in Ig and TCR loci and have been implicated in the accessibility control of V(D)J recombination (8). E-box sites are indeed present in iEκ and 3′Eκ, and it has been shown that E2A binds directly to these elements in vitro (9, 10) and in vivo (11). In addition, Vκ genes also contain E-boxes in their promoters and in close proximity to RSSs (12–15). Moreover, targeted mutation of the E-boxes, E1 and E2, in iEκ impairs *Igκ* rearrangement (16), directly demonstrating the functional importance of E-proteins in *Igκ* rearrangement during B cell development in vivo.

We have previously reported that enforced expression of E2A together with RAG1 and RAG2 in a nonlymphoid cell line BOSC23 can induce V(D)J recombination in endogenous *Igκ* and TCR loci (8, 17). In this system, ectopically expressed E2A proteins induced germline transcription of the Jκ gene region as well as the Vκ genes, indicating that E2A facilitated the recruitment of recombinase machinery to target gene segments by increasing chromatin accessibility. In addition, enforced E2A expression appeared not to induce the expression of other transcription factors that might promote the accessibility including EBF, Pax5, PU.1, Oct-2, and NF-κB, suggesting that E2A is likely to function directly to promote the accessibility of the *Igκ* locus. However, it is unclear whether E2A increases chromatin accessibility of target gene segments by direct binding to the gene segments or indirectly through the activation of the *Igκ* enhancers. Previous studies have also shown that E2A interacts with multiple histone acetyltransferase (HAT) complexes including p300, CBP, or SAGA (18–21). However, there is no evidence indicating that E2A has the ability to recruit these HAT complexes to target gene segments in vivo.

In the current study, we demonstrated that ectopically expressed E2A proteins in BOSC23 cells have the ability to bind directly to the Vκ gene promoter and RSS regions and to recruit CBP/p300 that promote histone acetylation, thereby increasing chromatin accessibility of target gene segments. Furthermore, these findings were also confirmed for endogenous E2A proteins in a mouse pre-B cell line.

Materials and Methods

Cell culture, plasmids, and transfection

BOSC23 cells were maintained in high-glucose DMEM supplemented with 10% FBS and antibiotics. The following expression plasmids have been previously described: pHβAPNeo, pHβAP E47, pEBB RAG1 and pEBB RAG2 (8), pCSretTAC AS3 and pCSretTAC E47 (22), pRc/RSV CBP-hemagglutinin (HA) (23), and pCMVβ p300-CHA (24). BOSC23 cells were plated at 2×10^6 cells per 6-cm dish 1 d before transfection and transfected using Lipofectamine and Plus Reagent (Invitrogen).

BKO84 cells were cultured in RPMI 1640 medium supplemented with 10% FCS, 5×10^{-7} M 2-mercaptoethanol and antibiotics (25). Retroviral vectors expressing a microRNA (miRNA)-based E2A knockdown construct or a negative control construct were generated as follows: oligonucleotides carrying an E2A target sequence or a LacZ control sequence were ligated into the pcDNA6.2-GW/miR vector (Invitrogen), and the resultant expression cassettes were transferred by Gateway Technology to the retroviral vector, MSCV GW PIG, which was generated by inserting the GW cassette into MSCV PIG dRI (26), kindly provided by Drs. S.W. Lowe and A. Yu (Howard Hughes Medical Institute, Memorial Sloan-Kettering Cancer Center [S.W.L.] and Cold Spring Harbor Laboratory [A.Y.]). Retroviral supernatants were prepared using the Plat-E packaging cell line (27), kindly provided by Dr. T. Kitamura (University of Tokyo). BKO84 cells were transduced with retroviruses and selected with 2 μg/ml puromycin after 2 d and used for assay at least after 7 d. Puromycin-resistant cells were cultured with 10 ng/ml PMA (Calbiochem) or vehicle control (DMSO) for 17 h (RT-PCR and chromatin immunoprecipitation assay) and 48 h (genomic PCR for rearrangement).

Abs

Abs were obtained from the following sources: normal rabbit IgG, anti-E2A (V-18X and N-649X), anti-CBP (451), anti-p300 (N-15), anti-GAPDH (Santa Cruz Biotechnology), anti–acetyl-histone H3 (K9 and K14), anti–acetyl-histone H4 (K5, K8, K12, and K16), anti–acetyl-histone H3K9, anti–acetyl-histone H3K14, anti–acetyl-histone H3K18, anti–acetyl-histone H3K23, anti–dimethyl-histone H3K4, anti–dimethyl-histone H3K9 serum (Upstate Biotechnology), anti–trimethyl-histone H3K4 (Abcam), anti-HA (HA-7) (Sigma-Aldrich), and anti–α-tubulin (CP06) (Calbiochem).

Quantitative RT-PCR analysis

Total RNA was isolated using TRIzol (Invitrogen), and contaminating genomic DNA was removed using DNA-free (Ambion). cDNA was synthesized using MMLV reverse-transcriptase Superscript III (Invitrogen) and Oligo $(dT)_{20}$ primer (Invitrogen). Transcript levels in BOSC23 cells were quantified by real-time PCR using QuantiTect SYBR Green PCR mix (Qiagen) on an Opticon2 DNA Engine (MJ Research), and transcript levels in BKO84 cells were quantified by real-time PCR using iQ SYBR Green Supermix (Bio-Rad) on a LightCycler 480 SystemII (Roche Applied Science) and normalized to β-actin mRNA.

PCR analysis of Igκ *rearrangement*

Genomic DNA was isolated as described (28). VκI-Jκ rearrangements in BOSC23 cells were quantified by real-time PCR as described for RT-PCR and normalized to the human CD14 gene. Vκ-Jκ rearrangements in BKO84 cells were analyzed by semiquantitative PCR as described (25).

Chromatin immunoprecipitation

For chromatin immunoprecipitation (ChIP) assays, BOSC23 cells were transfected with expression vectors pCSretTAC AS3 or pCSretTAC E47 as described earlier. Cells were harvested after 2 d posttransfection and positively selected for the expression of the TAC Ag (human CD25) using CD25 MicroBeads (Miltenyi Biotec). The purity of the enriched $CD25^+$ BOSC23 cell fraction was consistently >90%. ChIP assays were performed as described (28). Briefly, purified $CD25^+$ BOSC23 cells were fixed with 1% formaldehyde for 5–20 min at room temperature. Soluble chromatin was prepared from 1×10^6 to 3×10^6 fixed cells and immunoprecipitated with the Abs indicated earlier. DNA was purified from the bound and input fractions and quantified by real-time PCR as described for RT-PCR. For CBP/p300 ChIP using BOSC23 cells, purified DNA was amplified by ligation-mediated PCR (LM-PCR) for enhancement of the signals as described (29). ChIP assays using BKO84 cells transduced with retroviruses and selected with puromycin were performed similarly as described above.

Immunoblot analysis

Total cell lysates were analyzed by immunoblotting using anti-HA, anti-E2A, anti–α-tubulin, or anti-GAPDH Abs and the ECL Plus Western blotting detection system (Amersham Pharmacia Biotech). Images were captured and intensities of specific bands measured using an LAS-3000 imaging system (Fuji Film).

EMSA

Double-stranded oligonucleotides corresponding to the μE5 sequence in the intronic enhancer of the *IgH* gene and the OCT sequence in the promoter of the *Igκ* gene were end-labeled and used as probes. Nuclear extracts were prepared from transfected BOSC23 cells and analyzed for the binding activity to the μE5 or OCT probe as described (30). For supershift assays, nuclear extract was preincubated with 2 μg of control normal rabbit IgG or anti-E2A for 20 min at room temperature followed by the addition of the end-labeled probe. The mixture was incubated at room

temperature for 30 min and analyzed by PAGE. Images were captured and intensities of specific bands measured using a BAS-3000 imaging system.

Knockdown experiment using small interfering RNAs

For CBP and p300 knockdown in BOSC23 cells, Stealth Select RNA interference (RNAi) duplexes were designed within conserved sequences between CBP and p300 genes using BLOCK-iT RNAi Designer (Invitrogen). Three different sequences of RNAi duplexes were synthesized and mixed for use to minimize off-target effects. Stealth RNAi negative control duplexes (Invitrogen) or Stealth RNAi duplexes for PTP2cγ were used as a negative control. BOSC23 cells were plated at 1×10^6 cells per 6-cm dish 1 d before transfection and then transfected with mixed RNAi duplexes using Lipofectamine 2000 (Invitrogen). Twenty-four hours after RNAi transfection, the cells were transfected with various expression plasmids using Lipofectamine and Plus Reagent as described above. The cells were harvested 2 or 3 d after plasmid transfection.

LM-PCR for signal broken ends

LM-PCR analysis of signal broken ends (SBEs) at the Jκ1 gene segment was performed as described (8).

Sequences of the PCR primers and EMSA probes are available upon request.

Results

E2A binds to the regulatory regions in Igκ *locus and increases histone modifications associated with active transcription*

The presence of many E-box sites in the regulatory elements such as iEκ and 3′Eκ as well as Vκ gene promoters suggests that E2A increases accessibility by binding directly to these elements in the *Igκ* locus in vivo when transfected into BOSC23 cells. To test this possibility, we first assessed in vivo occupancy of ectopically expressed E2A proteins throughout the *Igκ* locus by ChIP assay using anti-E2A Abs. For these ChIP experiments, we used the expression vector for E2A and a human CD25 marker mediated by an internal ribosome entry site (pCSRetTAC E47) and the control vector (pCSRetTAC AS3) to purify the cells coexpressing the cell surface marker by magnetically sorting and used these purified cell populations (22). This strategy appeared to be useful particularly in histone ChIP described later, presumably because it avoids the dilution of histones specifically modified upon E2A expression with unmodified ones derived from non-E2A-expressing cells. Chromatin prepared from purified BOSC23 cells was immunoprecipitated with anti-E2A Abs and analyzed for the association with E2A by quantitative real-time PCR using various primer sets covering the VκI promoter, VκI RSS, Jκ1, Jκ2, or Jκ5 gene segment, iEκ, the Cκ, and 3′Eκ (Fig. 1A). Primers were designed within the consensus sequence to amplify the promoter and RSS regions of the multiple VκI gene family members, each having two canonical E-box sites (15). We sequenced cloned VκI gene segments in ChIP samples and confirmed that multiple VκI genes were indeed amplified by these primers (Supplemental Table I). In the absence of E2A overexpression, E2A binding was not detected throughout the locus, but upon E2A expression high levels of E2A binding were detected at the VκI promoter and the VκI RSS (Fig. 1B). A considerable level of E2A occupancy was also detected at iEκ and to a lesser extent at Jκ1 and 3′Eκ, consistent with the fact that these regions contain canonical E-box sites and E2A has the ability to bind these elements in vitro (9, 10, 12–15). Indeed, we identified 10 potential E-box sites in the consensus sequence of the VκI family members and the Jκ1 region and confirmed specific E2A binding to these potential E-box sites in vitro by EMSAs using nuclear extracts that were prepared from BOSC23 cells transfected with E2A (Supplemental Fig. 1).

To determine whether histone acetylation levels correlate with E2A occupancy, we next examined the histone acetylation status of the *Igκ* locus in BOSC23 cells with or without E2A expression by ChIP using Abs specific for diacetylated histone H3 lysines 9 and 14 (H3K9/14ac) and tetra-acetylated histone H4 lysine 5, 8, 12, and 16 (H4K5/8/12/16ac). Acetylation of H3 and H4 was considerably increased at the VκI promoter and RSS regions upon E2A expression, indicating that hyperacetylation of H3 and H4 correlates with the association of E2A (Fig. 1B). In contrast, we could not detect apparently elevated acetylation at iEκ, Jκ1, and 3′Eκ despite the possible association of E2A at these regions. This might be because there is a threshold of E2A occupancy sufficient to increase histone acetylation. Alternatively, the detection efficiency for histone acetylation at these regions, if any, might be still lower than that for E2A occupancy even after purification of E2A-expressing cells as described earlier. We also examined the histone methylation status of the *Igκ* locus by ChIP using Abs specific for methylated lysine residues on histone H3 including dimethylated lysine 4 (H3K4me2), trimethylated lysine 4 (H3K4me3), and dimethylated lysine 9 (H3K9me2). High levels of H3K4me2 and H3K4me3, but not H3K9me2, were detected at VκI promoter and RSS upon E2A overexpression (Fig. 1B). These results indicated that histone modifications associated with active transcription such as acetylation and H3K4me2 and H3K4me3, but not H3K9me2, were accompanied with the binding of E2A to the chromatin in a region specific manner.

E2A recruits histone acetyltransferase p300 and CBP at the VκI promoter and RSS regions

Given that E2A has been shown directly to interact with p300 and CBP, transcriptional coactivators harboring histone acetyltransferase activity (18, 19, 21), we considered the possibility that p300/CBP are recruited by E2A to increase histone acetylation in vivo. To test this, we performed similar ChIP analyses using Abs recognizing p300 and CBP. In the absence of E2A overexpression, association of E2A itself, p300, or CBP was not detected at either the VκI promoter or RSS regions (Fig. 1C). However, enforced E2A expression induced association of p300 and CBP with chromatin at the VκI promoter and RSS regions in accord with the binding of E2A, suggesting that E2A has the ability to recruit p300/CBP to the VκI promoter and RSS regions to increase histone acetylation (Fig. 1C). Consistent with the finding that the increase in histone acetylation at the Jκ regions was not detectable upon E2A overexpression, we could not detect the association of p300 and CBP at the Jκ regions (data not shown). Therefore, we focused on the VκI promoter and RSS regions in further analyses.

Exogenous p300 and CBP facilitate E2A-induced histone hyperacetylation at the VκI promoter and RSS regions

We next sought to determine whether CBP/p300 are functionally involved in the elevation of histone acetylation at the VκI promoter and the VκI RSS upon E2A expression. For this purpose, we overexpressed p300 and CBP along with E2A in BOSC23 cells and assessed histone acetylation levels at the VκI promoter and RSS regions by ChIP assays. In initial attempts, we could not observe any changes in histone H3 acetylation upon CBP/p300 overexpression by using Abs against H3K9/14ac. Because CBP/p300 have been reported to acetylate preferentially K14, K18, and K23 on histone H3 in vitro (31), we sought to dissect the acetylation status of the individual lysine residues on histone H3 by using Abs specific to acetylated H3K9, H3K14, H3K18, and H3K23. Consistent with the elevated histone H3 acetylation detected by Abs specific for H3K9/14ac, E2A overexpression alone increased acetylated histone H3 lysine 9 (H3K9ac) levels and to a lesser extent acetylated histone H3 lysine 18 (H3K18ac) levels both at VκI promoter and VκI RSS (Fig. 2). Coexpression of CBP/p300 together with E2A led to further enhancement of H3K18ac, but not H3K9ac (Fig. 2). Although acetylated histone

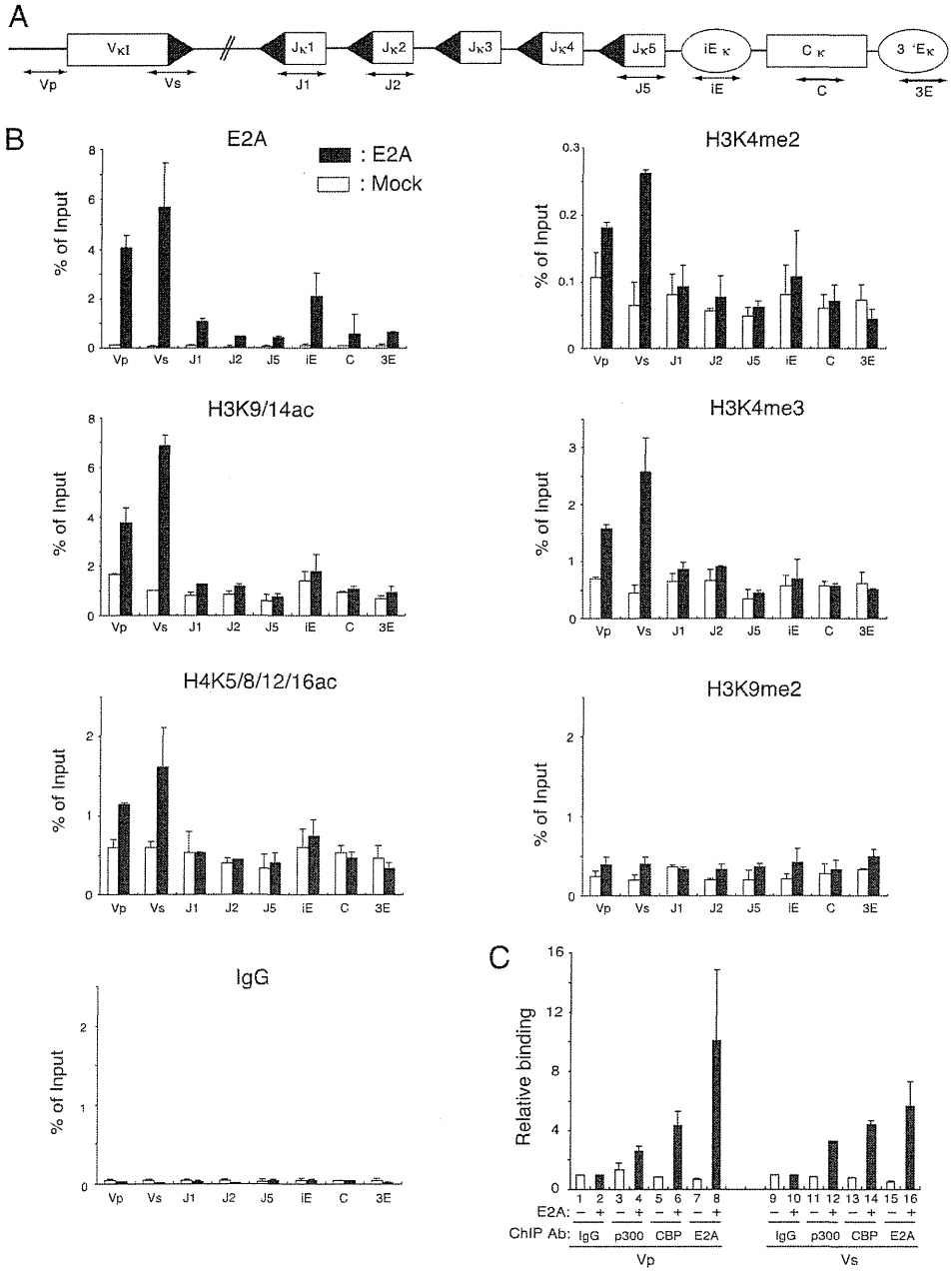

FIGURE 1. E2A binds to the regulatory regions in the *Igκ* locus and acts to increase histone acetylation by recruiting CBP/p300. (**A**) A schematic diagram of the human *Igκ* locus. Boxes, triangles, and ellipses represent gene segments, RSSs, and enhancer regions, respectively. Locations of the amplified regions in ChIP analysis are shown below the diagram: VκI promoter (Vp), VκI RSS (Vs), Jκ1, Jκ2, Jκ5 gene segment (J1, J2, J5), iEκ (iE), C region gene (C), and 3′Eκ (3E). (**B**) ChIP analysis of E2A binding and histone modification in the *Igκ* locus of BOSC23 cells transfected with E2A (black bar) or mock plasmid (white bar). Chromatin was prepared from transfected BOSC23 cells enriched for CD25 coexpression marker and immunoprecipitated with Abs against E2A, H3K9/14ac, H4K5/8/12/16ac, H3K4me2, H3K4me3, H3K9me2, or control normal rabbit IgG. The bound and input fractions were quantified by real-time PCR, and ratios of bound/input are indicated as a percentage of input for each region. Data are the mean of duplicate PCRs with range and are representative of two independent experiments. (**C**) ChIP analysis of E2A, p300, and CBP binding to VκI promoter and VκI RSS regions in BOSC23 cells transfected with E2A (black bar) or mock plasmid (white bar). Chromatin was prepared from transfected BOSC23 cells enriched for CD25 coexpression marker and immunoprecipitated with control normal rabbit IgG or Abs against p300, CBP, or E2A. Note that this anti-CBP Ab also cross-reacts with p300 as indicated in Fig. 6A. The recovered DNA was amplified by LM-PCR for enhancement of the signals. The amplified DNA from bound fractions was quantified by real-time PCR with primers for the Vp and Vs regions, and binding levels were normalized to input levels, and relative binding levels were normalized to binding levels with IgG and are shown as the mean of duplicate PCRs with range. Data are representative of two independent experiments.

H3 lysine 14 (H3K14ac) and acetylated histone H3 lysine 23 (H3K23ac) exhibited high basal levels compared with H3K9ac and H3K18ac prior to transfection, H3K14ac and H3K23ac levels were not elevated by transfection of E2A alone or E2A plus CBP/p300 (Fig. 2). This is consistent with previous findings that H3K14ac could be detected prior to estrogen-stimulated transcription of the *pS2* gene and that H3K14ac levels did not change during the estrogen stimulation (32). These results suggest that CBP/p300 play functional roles in E2A-induced acetylation of histone H3, at least on K18, at the VκI promoter and RSS regions.

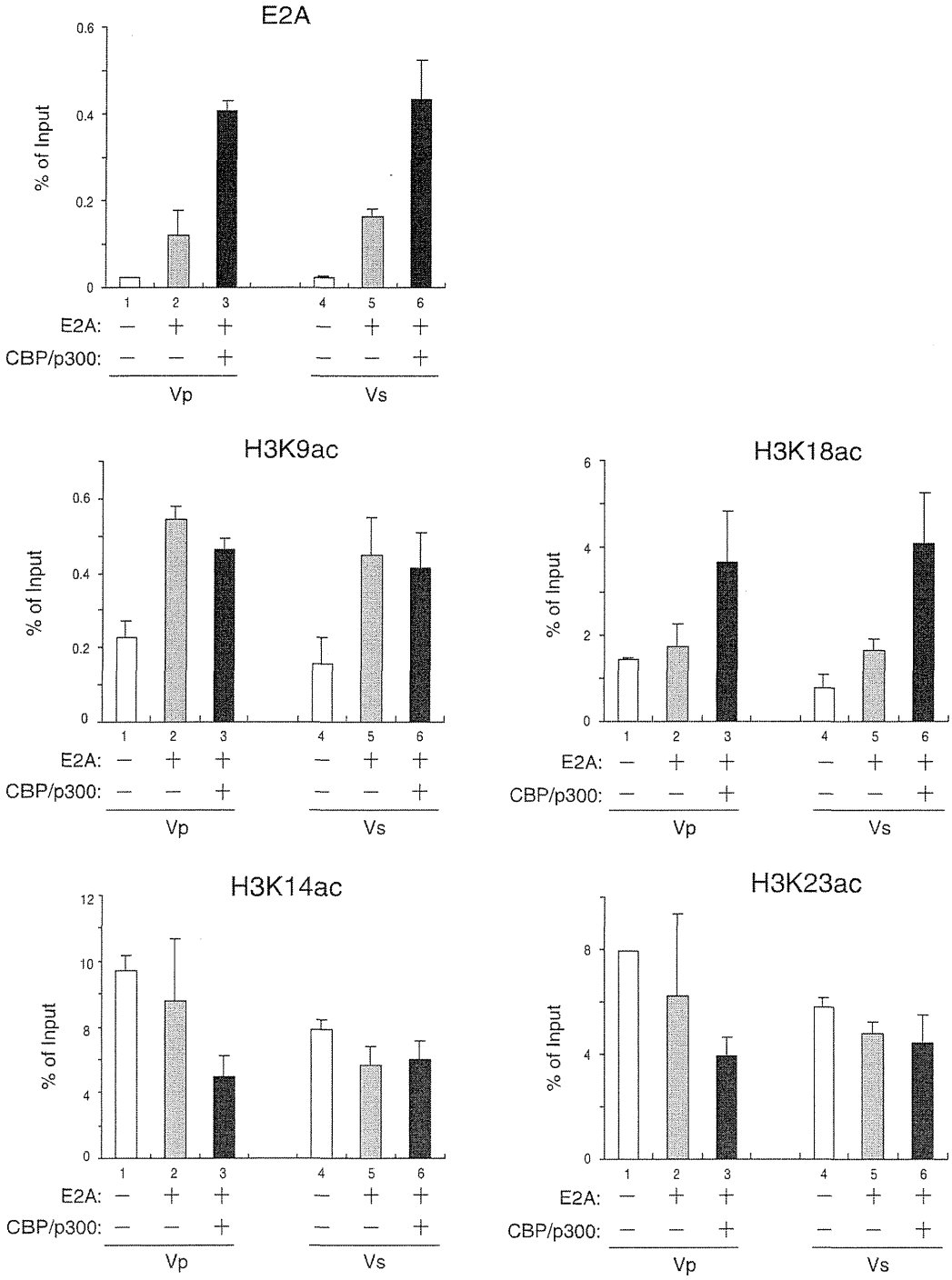

FIGURE 2. Overexpression of CBP/p300 enhances E2A-induced histone H3K18 acetylation at the Vκ*I* promoter and RSS regions. ChIP analysis of E2A binding and histone acetylation at the Vκ*I* promoter and Vκ*I* RSS regions in BOSC23 cells transfected with mock plasmid (white bar), E2A alone (gray bar), and E2A and CBP/p300 (black bar). Chromatin was prepared from transfected BOSC23 cells enriched for CD25 coexpression marker and immunoprecipitated with Abs against E2A, H3K9ac, H3K14ac, H3K18ac, and H3K23ac. The bound and input fractions were quantified by real-time PCR with primers for the Vκ*I* promoter (Vp) and Vκ*I* RSS (Vs) regions, and ratios of bound/input are indicated as a percentage of input for each region. Data are the mean of duplicate PCRs with range and are representative of two independent experiments.

Notably, overexpression of CBP/p300 led to the increased association of E2A with chromatin at Vκ*I* promoter and Vκ*I* RSS (Fig. 2). Immunoblot analyses using an anti-E2A Ab revealed that coexpression of CBP/p300 did not change the abundance of overexpressed E2A proteins (Fig. 3A). In addition, EMSA using an E-box site in the *IgH* intronic enhancer, μE5, as a probe revealed that the binding activity of E2A proteins to the naked-DNA μE5 probe was not increased upon overexpression of CBP or p300 (Fig. 3B). Taken together, these results suggest that the chromatin structural changes including H3K18ac promoted by CBP/p300 play a critical role in increased E2A association with Vκ*I* chromatin. Alternatively, E2A binding onto Vκ*I* chromatin might be stabilized by the formation of the complex with CBP/p300.

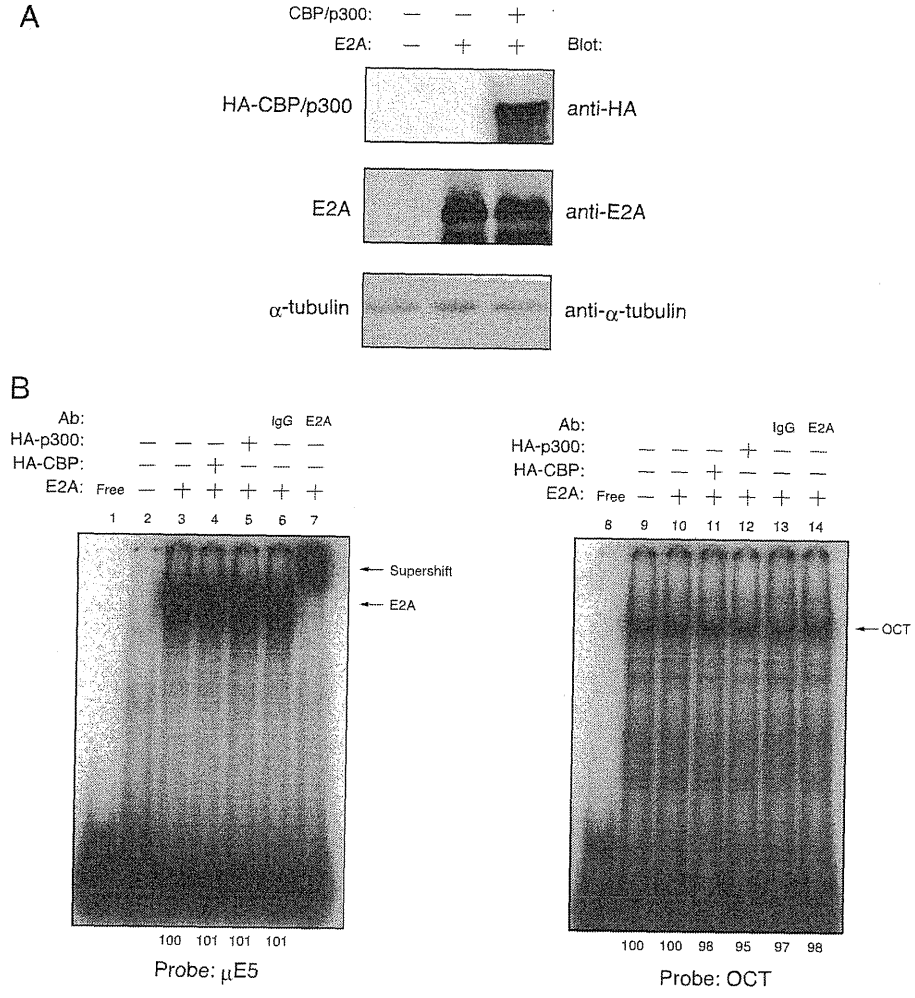

FIGURE 3. Overexpression of CBP/p300 does not affect E2A protein abundance and DNA binding activity. (**A**) Immunoblot analysis of E2A protein abundance in BOSC23 cells transfected with mock plasmid, E2A alone, and E2A plus CBP/p300. ChIP lysates used for the analysis shown in Fig. 2 were analyzed for the expression levels of the HA-tagged CBP/p300, E2A, and α-tubulin proteins by immunoblotting using anti-HA, anti-E2A, and anti–α-tubulin Abs, respectively. Intensities of specific bands were measured with a densitometer. (**B**) EMSA analysis of E2A DNA binding activity in transfected BOSC23 cells. Nuclear extracts were prepared from BOSC23 cells transfected with mock plasmid, E2A alone, E2A plus HA-CBP, or E2A plus HA-p300 and analyzed for the binding activity to the μE5 (*left panel*) or OCT (*right panel*) probe. Free probes were run in *lanes 1* and *8* ("Free"). The specificity of E2A DNA binding complex was examined using control normal rabbit IgG or an anti-E2A Ab (E2A). The specific binding complexes and supershifted complexes are indicated. Intensities of specific bands were measured with a densitometer, and relative intensities to E2A alone (μE5) and to without E2A (OCT) are indicated as percentages. Data are representative of two independent experiments.

Overexpression of CBP/p300 enhances E2A-induced Vκ germline transcription and Igκ *rearrangement in BOSC23 cells*

We previously reported that enforced E2A expression induces germline transcription (GLT) of the VκI genes and also synergizes with RAG1/2 to induce VκI-Jκ recombination of the endogenous *Igκ* locus in BOSC23 cells (8). Again, we sequenced cloned VκI genes in GLT samples and confirmed that multiple VκI genes were amplified and most of them overlapped with the ones that were found in the H3K9/14ac ChIP samples (Supplemental Table I). Thus, we next examined whether overexpression of CBP/p300 affects E2A-induced VκI GLT and VκI-Jκ rearrangement by quantitative real-time PCR (Fig. 4A). Overexpression of CBP or p300 resulted in 1.7- to 2.3-fold increases of VκI GLT and 5.2- to 7.4-fold increases of VκI-Jκ rearrangement compared with E2A alone, respectively (Fig. 4B, 4C). Moreover, increasing amounts of CBP/p300 expression vectors led to graded responses in Vκ GLT and VκI-Jκ rearrangement (Supplemental Fig. 2). Together, these results demonstrate that CBP/p300 are recruited to the VκI promoter and RSS regions by E2A and play a critical role in the elevation of H3K18ac and E2A occupancy, which are closely associated with the increases of VκI GLT and VκI-Jκ rearrangement.

Knockdown of CBP/p300 leads to decreases in histone acetylation and E2A binding to the VκI chromatin

To confirm the functional importance of CBP/p300 in the E2A-mediated increase of histone acetylation at the VκI promoter and RSS chromatin, we used RNAi to reduce the endogenous expression of CBP/p300 (Fig. 5). For this purpose, we designed small interfering RNAs (siRNAs) targeted to conserved sequences in CBP and p300. A similar strategy has been reported successfully to reduce the level of bulk histone H3K18 (33). Immunoblot analyses showed that the siRNA for CBP/p300 reduced the expression levels of endogenous p300 and CBP proteins to less than 10 and 20% of those in untransfected cells, respectively (Fig. 6A).

To assess the functional roles for CBP/p300 in the E2A-mediated induction of histone acetylation, siRNA-transfected BOSC23 cells were transfected again with a vector expressing E2A or an empty vector 24 h after siRNA transfection. E2A-expressing cells were purified by cell sorting 3 d after siRNA transfection and analyzed for histone acetylation by ChIP assays. Knockdown of CBP/p300 markedly diminished the E2A-induced acetylation of H3K9 and H3K18 at both the VκI promoter and RSS regions but did not affect acetylation of K14 and K23 (Fig. 5), indicating that endogenous CBP/p300 are functionally required for the E2A-induced acetylation.

As opposed to the overexpression of CBP/p300, knockdown of CBP/p300 reduced the levels of E2A occupancy at both the VκI promoter and RSS regions to ~15% of those in control siRNA-treated cells (Fig. 5) and also at other regions in the *Igκ* locus including iEκ, indicating that this is a general phenomenon (Supplemental Fig. 3). Immunoblot analyses showed that knockdown of CBP/p300 did not affect the E2A protein levels (Fig. 6A). In addition, EMSA analyses indicated that the binding activity of

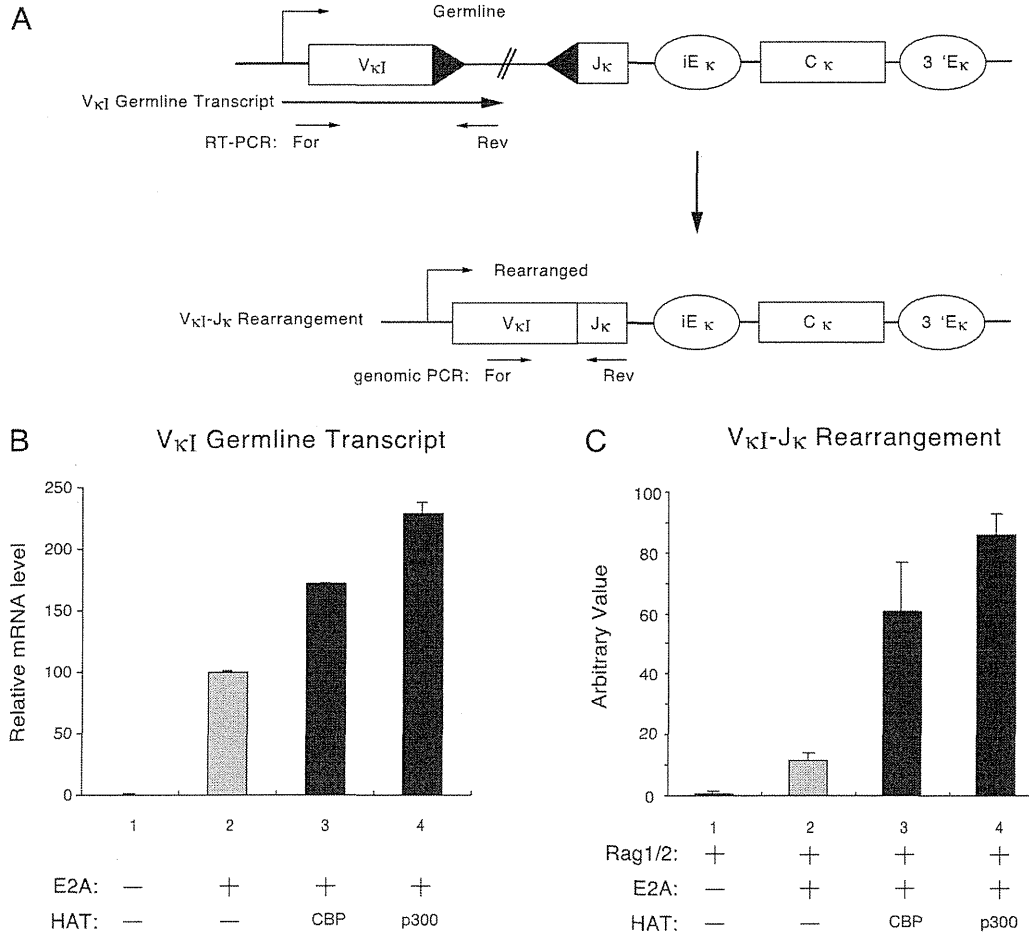

FIGURE 4. Overexpression of CBP/p300 enhances E2A-induced VκI GLT and VκI-Jκ rearrangement. (**A**) A schematic diagram of detection for VκI GLT and VκI-Jκ rearrangement. Boxes, triangles, and ellipses represent gene segments, RSSs, and enhancer regions, respectively. Locations of forward ("For") and reverse ("Rev") primers used for RT-PCR and genomic PCR are indicated as arrows. (**B**) RT-PCR analysis of VκI GLT. RNA was isolated from BOSC23 cells transfected with indicated expression plasmids and analyzed for VκI GLT by real-time RT-PCR using primers shown in (A). VκI GLT levels were normalized to β-actin mRNA levels, and relative mRNA levels are shown as the mean of duplicate PCRs with range. Data are representative of three independent experiments. (**C**) Genomic PCR analysis of VκI-Jκ rearrangement. Genomic DNA was isolated from BOSC23 cells transfected with indicated expression plasmids and analyzed for VκI-Jκ rearrangement by real-time PCR using primers shown in (A). VκI-Jκ rearrangement levels were normalized to the CD14 gene, and normalized rearrangement levels in arbitrary values are shown as the mean of duplicate PCRs with range. Data are representative of three independent experiments.

E2A to naked DNA was not changed by CBP/p300 knockdown (Fig. 6B). These data therefore suggest that CBP/p300 regulate in vivo binding of E2A to the VκI promoter and RSS regions at the chromatin level in conjunction with acetylation of H3K9 and H3K18. It is conceivable that the reduction in acetylation of H3K9 and H3K18 by CBP/p300 knockdown is simply caused by the reduction of the E2A occupancy. However, it should be noted that knockdown of CBP/p300 did not completely abrogate the E2A occupancy at the VκI promoter and RSS regions; rather, residual levels of E2A binding remained (Fig. 5). Nonetheless, the reduction of H3K9 and H3K18 acetylation by CBP/p300 knockdown was complete, suggesting that knockdown of CBP/p300 directly affected acetylation of H3K9 and H3K18 beyond the E2A occupancy.

Knockdown of CBP/p300 reduces E2A-induced Vκ GLT and Igκ rearrangement in BOSC23 cells

We examined whether endogenous CBP/p300 are indeed functionally required for E2A-induced VκI GLT and VκI-Jκ rearrangement. Knockdown of CBP/p300 resulted in a reduction of E2A-induced VκI GLT and VκI-Jκ rearrangement to ~56 and 41% of those in control siRNA-treated cells, respectively (Fig. 7A, 7B). To confirm further the reduced VκI-Jκ rearrangement by CBP/p300 knockdown, we also analyzed SBEs at the Jκ1 gene segment, which are the hallmark of de novo gene rearrangement and accessibility, by using LM-PCR (34). Considerable levels of Jκ1 SBEs were detectable in cells transfected with either negative-control siRNA or no siRNA upon E2A overexpression; however, the level of Jκ1 SBEs was markedly decreased by siRNA for CBP/p300 (Fig. 7C). These results clearly indicate that endogenous CBP/p300 are functionally essential for E2A-induced accessibility and rearrangement at the *Igκ* locus.

E2A binds to a distinct set of Vκ genes and the regulatory regions in Igκ *locus in a mouse pre-B cell line*

In the experiments described earlier, we used the ectopic system with BOSC23 cells and found that the E2A proteins have the ability to bind directly to the Vκ promoter and RSS regions and to recruit CBP/p300, thereby increasing chromatin accessibility. It has been proposed that E2A binds to E-box sites around Vκ genes; however, there is no formal report showing direct E2A binding to Vκ genes in vivo. Thus, we sought to determine whether similar

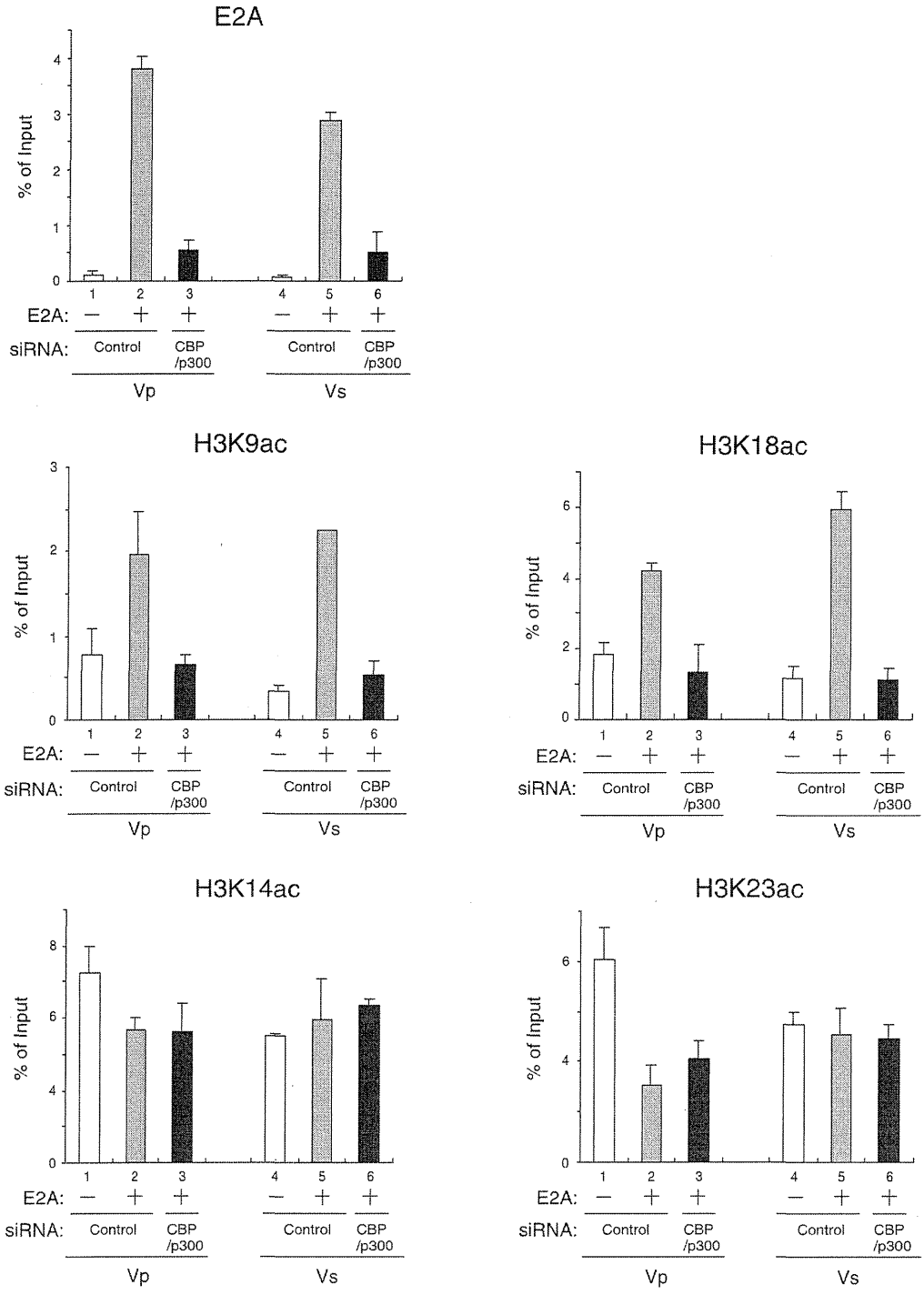

FIGURE 5. Knockdown of CBP/p300 reduces E2A-induced acetylation of histone H3K9 and H3K18 at Vκ1 promoter and Vκ1 RSS. ChIP analysis of E2A binding and histone acetylation at the Vκ1 promoter and Vκ1 RSS regions in BOSC23 cells transfected with mock plasmid and negative control siRNA (white bar), E2A and negative control siRNA (gray bar), and E2A and CBP/p300-specific siRNA (black bar). Chromatin was prepared from transfected BOSC23 cells enriched for CD25 coexpression marker and immunoprecipitated with Abs against E2A, H3K9ac, H3K14ac, H3K18ac, and H3K23ac. The bound and input fractions were quantified by real-time PCR with primers for the Vκ1 promoter (Vp) and Vκ1 RSS (Vs) regions, and ratios of bound/input are indicated as a percentage of input for each region. Data are the mean of duplicate PCRs with range and are representative of two independent experiments.

findings to those obtained with BOSC23 cells are also observed under more physiological conditions, including mouse pre-B cells.

To this end, we used a pre-B cell line, BKO84, derived from a mouse deficient in BLNK, also called BASH/SLP-65, which is an adapter protein critical for transmitting the pre-BCR signaling (25). BKO84 cells are developmentally arrested at the large pre-B cell stage due to the defect in *IgL* gene rearrangement. However, upon reconstitution of BLNK or treatment with PMA, which activates downstream signaling of the pre-BCR, BKO84 cells are induced to express IRF4, which is required for efficient activation of Jκ GLTs and rearrangement of *Igκ* locus (35, 36), and indeed BKO84 cells consequently undergo Vκ-Jκ rearrangement (25, 37). Using

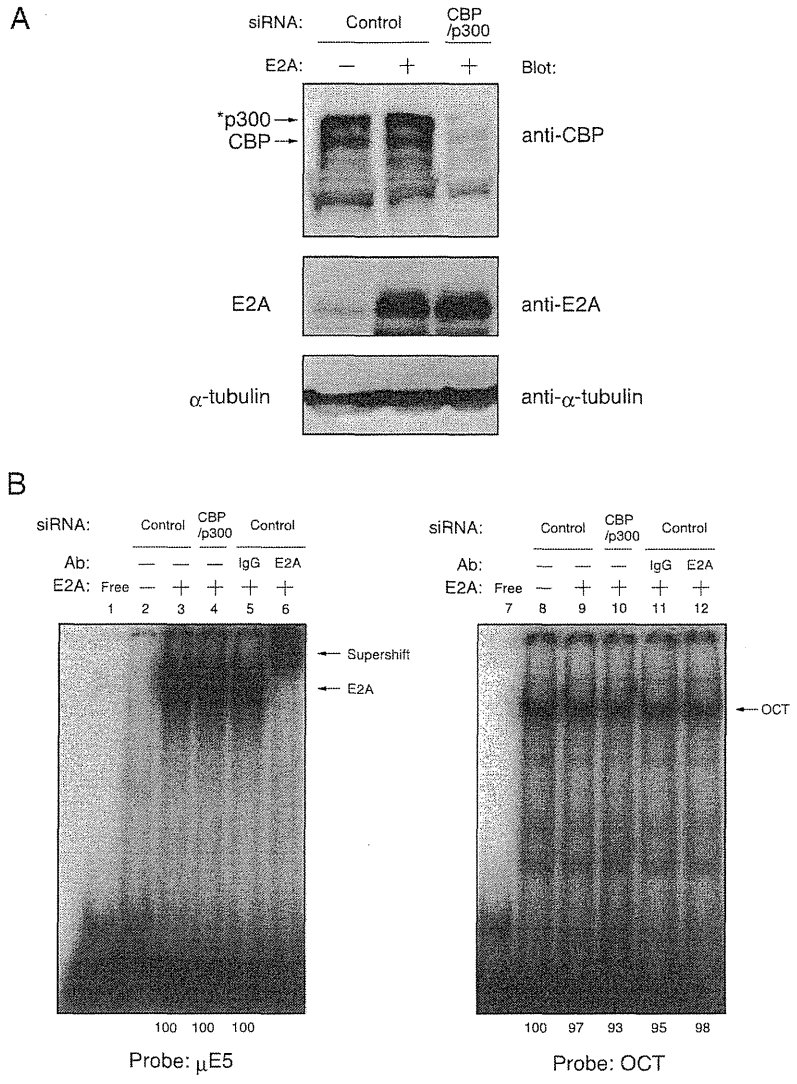

FIGURE 6. Knockdown of CBP/p300 does not affect E2A protein abundance and DNA binding activity. (**A**) Immunoblot analysis of E2A protein abundance in BOSC23 cells transfected with mock plasmid and negative control siRNA, E2A and negative control siRNA, and E2A and CBP/p300-specific siRNA. ChIP lysates used for the analysis shown in Fig. 5 were analyzed for the expression levels of endogenous CBP/p300, E2A, and α-tubulin proteins by immunoblotting using anti-CBP, anti-E2A, and anti–α-tubulin Abs, respectively. Note that the anti-CBP Ab cross-reacts with p300 as indicated by an asterisk. Intensities of specific bands were measured with a densitometer. (**B**) EMSA analysis of E2A DNA binding activity in BOSC23 cells transfected with mock or E2A expression plasmid and negative-control or CBP/p300-specific siRNA as indicated. Nuclear extracts were prepared from transfected BOSC23 cells and analyzed for the binding activity to the μE5 (*left panel*) or OCT (*right panel*) probe. Free probes were run in *lanes 1* and *8* ("Free"). The specificity of E2A DNA binding complex was examined using control normal rabbit IgG or anti-E2A Ab (E2A). The specific binding complexes and supershifted complexes are indicated. Intensities of specific bands were measured with a densitometer, and relative intensities to E2A alone (μE5) and to without E2A (OCT) are indicated as percentages. Data are representative of two independent experiments.

this BKO84 cell line, we first assessed in vivo E2A occupancy around several Vκ gene segments, Jκ GLT promoter, Jκ1 gene segment, iEκ, and 3′Eκ in the mouse *Igκ* locus as well as the mb-1 and α-actin promoter as a positive and negative control, respectively, by ChIP assay using anti-E2A Abs (Fig. 8A). These Vκ genes include the ones that were previously analyzed, and their accessibility has been shown to be dependent on iEκ (38). To analyze simultaneously the possible role for E2A in inducing accessibility, we tried to knock down E2A expression by transducing BKO84 cells with retrovirus expressing a miRNA-based E2A knockdown construct or a negative control construct. In unstimulated BKO84 cells expressing negative control miRNA, we detected considerable levels of E2A binding at iEκ, 3′Eκ, and mb-1 promoter, but not at α-actin promoter (Fig. 8B), as reported previously for the Abl-transformed pre-B cell line (39). After PMA treatment, the E2A binding level was increased at iEκ and 3′Eκ. This might be caused by the slight elevation of the E2A proteins and mRNA upon PMA stimulation (Figs. 8C, 9A). Among Vκ genes tested, we observed variable levels of E2A occupancy from considerable levels at Vκ11-127, Vκ9-120, and Vκ9-96 to a marginal level at Vκ4-54. Upon PMA treatment, E2A binding was substantially increased at the Vκ genes that exhibited considerable levels of E2A occupancy without PMA, but not at Vκ4-54. E2A binding levels were relatively low at the Jκ promoter and Jκ1 gene segment and not increased by PMA treatment. We next examined BKO84 cells expressing the E2A-specific miRNA and found that the E2A protein and mRNA abundance was successfully reduced in these cells compared with those in cells expressing negative control miRNA both in the absence or presence of PMA (Figs. 8C, 9A). E2A knockdown substantially reduced the E2A binding levels at most of the regions examined both with or without PMA, although some residual E2A binding levels were detected roughly proportional to the basal levels (Fig. 8B).

E2A acts to increase histone acetylation by recruiting p300 in a mouse pre-B cell line

To determine whether histone acetylation levels correlate with E2A occupancy in BKO84 cells, we next assessed H3K18ac levels in mouse *Igκ* locus (Fig. 8B), as H3K18ac levels are correlated well with CBP/p300 recruitment upon E2A overexpression in BOSC23 cells as described earlier. Although even in the absence of PMA, considerable levels of H3K18ac were detectable, PMA stimulation substantially increased H3K18ac levels at most of the regions in *Igκ* locus examined, but not at the α-actin promoter. E2A knockdown effectively inhibited PMA-induced H3K18ac elevation at most of the Vκ genes except Vκ4-54, which showed marginal E2A binding among Vκ genes. At the Vκ4-54 gene, basal and PMA-induced H3K18ac levels were not reduced, but

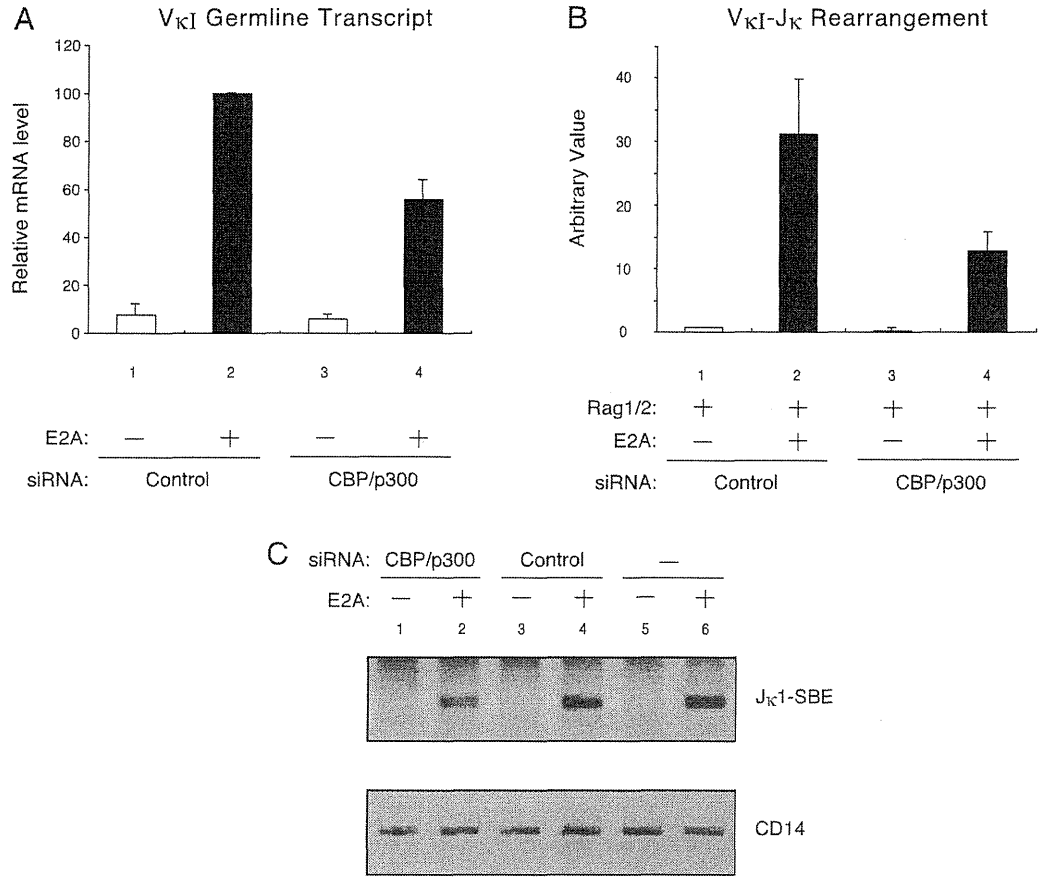

FIGURE 7. Knockdown of CBP/p300 expression reduces E2A-induced VκI GLT and VκI-Jκ rearrangement. (**A**) RT-PCR analysis of VκI GLT. RNA was isolated from BOSC23 cells transfected with indicated expression vectors and PTP2cγ-specific siRNA (Control) or CBP/p300-specific siRNA (CBP/p300) and analyzed for VκI GLT by real-time RT-PCR using primers as shown in Fig. 4A. VκI GLT levels were normalized to β-actin mRNA levels. Relative mRNA levels are shown as the mean of duplicate PCRs with range. Data are representative of three independent experiments. (**B**) Genomic PCR analysis of VκI-Jκ rearrangement. Genomic DNA was isolated from BOSC23 cells transfected with indicated expression plasmids and PTP2cγ-specific siRNA (Control) or CBP/p300-specific siRNA (CBP/p300) and analyzed for VκI-Jκ rearrangement by PCR using primers shown in Fig. 4A. VκI-Jκ rearrangement levels were normalized to the CD14 gene, and normalized rearrangement levels are shown as the mean of duplicate PCRs with range. Data are representative of three independent experiments. (**C**) LM-PCR analysis of SBEs at the Jκ1 gene segment. Genomic DNA was isolated from BOSC23 cells transfected with indicated expression plasmids and CBP/p300-specific siRNA (CBP/p300), PTP2cγ-specific siRNA (Control), or without siRNA (−) and analyzed for Jκ1 SBEs by LM-PCR. The CD14 gene was used as a loading control. Data are representative of two independent experiments.

rather increased by E2A knockdown, suggesting that Vκ4-54 is regulated by other factors than E2A and such factors may compete for HATs with E2A. In addition to Vκ genes, E2A knockdown also partially suppressed the PMA-induced H3K18ac increase at the Jκ promoter and Jκ1 gene segment. Because E2A binding around the Jκ region was not so apparent, the reduction in PMA-induced H3K18ac by E2A knockdown might be due to an indirect effect, presumably via iEκ and 3′Eκ to which E2A binds. Basal and PMA-induced H3K18ac levels at iEκ and 3′Eκ did not change upon E2A knockdown, despite the reduced E2A binding at these enhancers, suggesting that other factors that bound these enhancers might compensate for E2A to increase H3K18ac levels.

Furthermore, to determine whether the reduction of H3K18ac upon E2A knockdown correlates with a reduction of p300/CBP recruitment, we examined p300 recruitment by ChIP (Fig. 8D). Although the efficiency of p300 ChIP is not so high, we reproducibly detected specific p300 recruitment to at least three Vκ genes including Vκ11-127, Vκ9-120, and Vκ9-96, which exhibited high E2A binding. p300 occupancy was increased upon PMA treatment, and the increased p300 occupancy was reduced by E2A knockdown, indicating that E2A is required for the recruitment of p300 that is responsible for H3K18ac. Together, these data indicate that E2A binds to some Vκ genes and regulatory regions in the mouse *Igκ* locus and acts to increase histone acetylation by recruiting p300, confirming the similar findings observed with BOSC23 cells.

Knockdown of E2A reduces PMA-induced Vκ and Jκ GLT and Igκ *rearrangement in BKO84 cells*

Thus, we next examined whether E2A knockdown has an effect on Vκ and Jκ GLTs by quantitative RT-PCR (Fig. 9B). GLTs of Vκ and Jκ1 genes were low before PMA stimulation, but were strongly upregulated after PMA stimulation. In good correlation with changes in the H3K18ac levels, E2A knockdown led to a substantial reduction of PMA-induced Vκ and Jκ1 GLTs, except that Vκ4-54 GLT was not suppressed, but rather increased by E2A knockdown.

We finally tested whether endogenous E2A is required for Vκ-Jκ rearrangement. Semiquantitative genomic PCR analyses showed that E2A knockdown resulted in a reduction of PMA-induced Vκ-Jκ rearrangement compared with those in control miRNA-treated cells (Fig. 9C). We also analyzed expression of the genes involved in *Igκ* rearrangement and found that IRF4 is similarly upregulated by PMA even upon E2A knockdown, whereas IRF8 mRNA is slightly de-

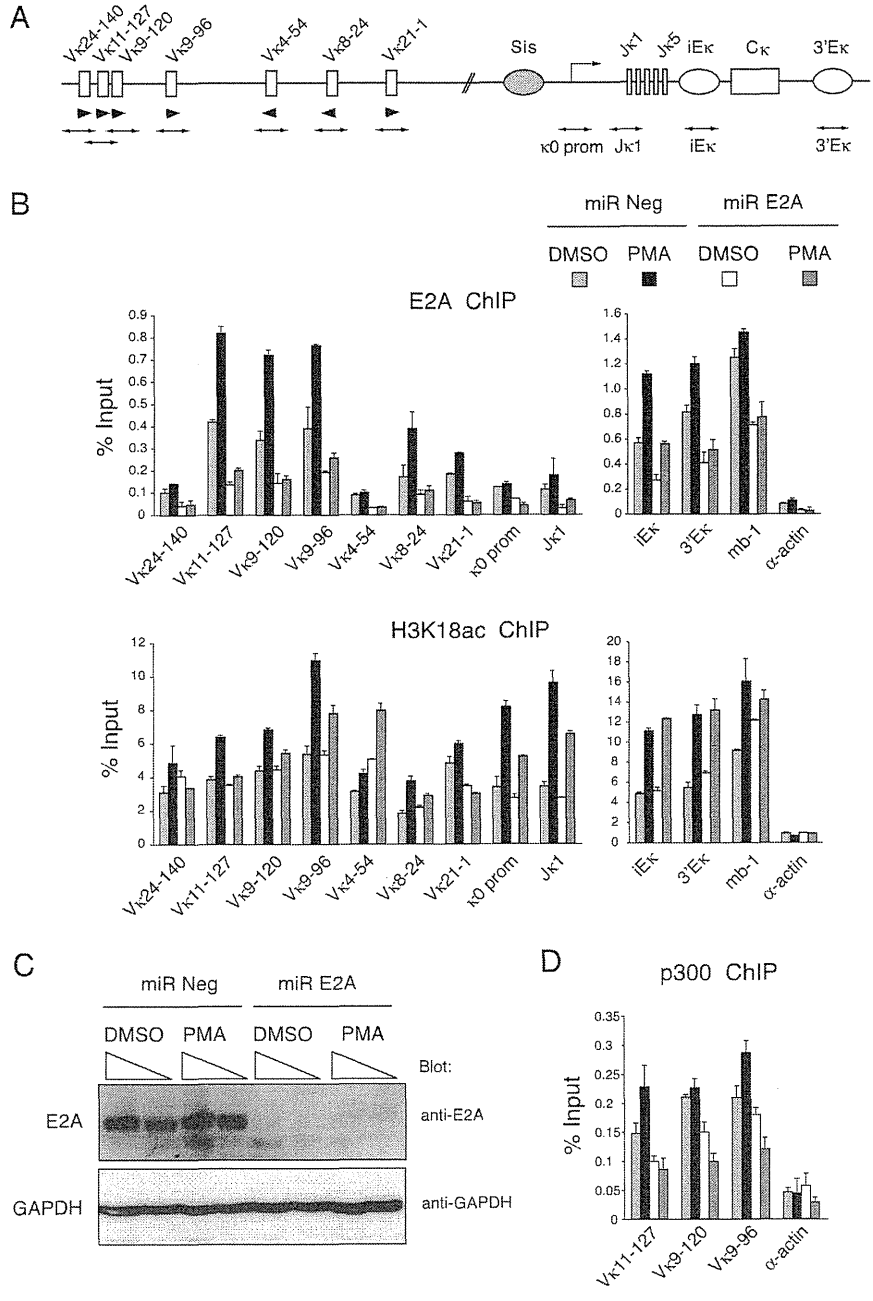

FIGURE 8. E2A binds to Vκ genes and regulatory regions in the mouse *Igκ* locus and acts to increase histone acetylation by recruiting p300. (**A**) A schematic diagram of the mouse *Igκ* locus. Boxes and ellipses represent gene segments and regulatory regions including the Sis element and enhancers, respectively. Relative positions and transcriptional orientations (arrowheads) of Vκ genes are indicated. Approximate locations of the amplified regions in ChIP analysis are shown below the diagram. (**B**) ChIP analysis of E2A binding and histone acetylation in the *Igκ* locus of BKO84 cells. Chromatin was prepared from BKO84 cells transduced with retrovirus expressing negative control miRNA or E2A-specific miRNA in the absence (DMSO) or presence of PMA and immunoprecipitated with Abs against E2A and H3K18ac. The bound and input fractions were quantified by real-time PCR, and ratios of bound/input are indicated as a percentage of input for each region. Data are the mean of triplicate PCRs with SD and are representative of three independent experiments. (**C**) Immunoblot analysis of E2A protein abundance in BKO84 cells transduced as in (B). Whole-cell lysates used for the analysis shown in (B) were analyzed using anti-E2A and anti-GAPDH Abs, respectively. (**D**) ChIP analysis of p300 occupancy in the *Igκ* locus of BKO84 cells. ChIP was performed as in (B) using anti-p300 Ab. κ0 prom, Jκ promoter.

creased by E2A knockdown (Fig. 9A). Given that these genes are functionally redundant (36), the reduction of Vκ-Jκ rearrangement by E2A knockdown is unlikely due to the decreased IRF8 expression. Rag1/2 mRNA levels were also upregulated by PMA partly due to a slight increase of Foxo1 mRNA (Fig. 9A). Notably, Rag1/2 mRNA levels were not decreased but rather markedly increased by E2A knockdown (Fig. 9A). It was recently reported that Rag expression is negatively regulated by Gfi1b (40) and also that Gfi1b expression is positively regulated by E2A (41, 42). We thus assessed Gfi1b mRNA expression and found that E2A knockdown led to a reduction in Gfi1b mRNA levels, suggesting that the increased Rag expression upon E2A depletion is likely due to the reduced Gfi1b expression. Together, these results suggest that the reduction of Vκ-Jκ rearrangement by E2A knockdown is not caused by alteration of Rag1/2 expression but likely due to the reduced accessibility of the Vκ and Jκ gene segments.

Discussion

In the current study, we used the ectopic expression system using BOSC23 cells and demonstrated that ectopically expressed E2A proteins have the ability to bind directly to the Vκ promoter and RSS regions and to recruit CBP/p300, which promote histone acetylation, thereby increasing chromatin accessibility of target gene segments.

In contrast to the regulation of Jκ region accessibility by the *Igκ* enhancers, the regulation of Vκ gene accessibility is not well understood. However, extensive sequence analyses of the human and mouse *Igκ* loci have revealed that octamer motifs and E-box sites are highly conserved in almost all Vκ gene promoters (12–15). In addition to the promoters, potential binding sites for transcription factors including E2A are also present in the intron of Vκ genes and downstream of RSSs. Indeed, we showed that E2A has the ability to bind directly to the conserved E-box site present downstream of Vκ RSSs and to increase histone acetylation at these regions in BOSC23

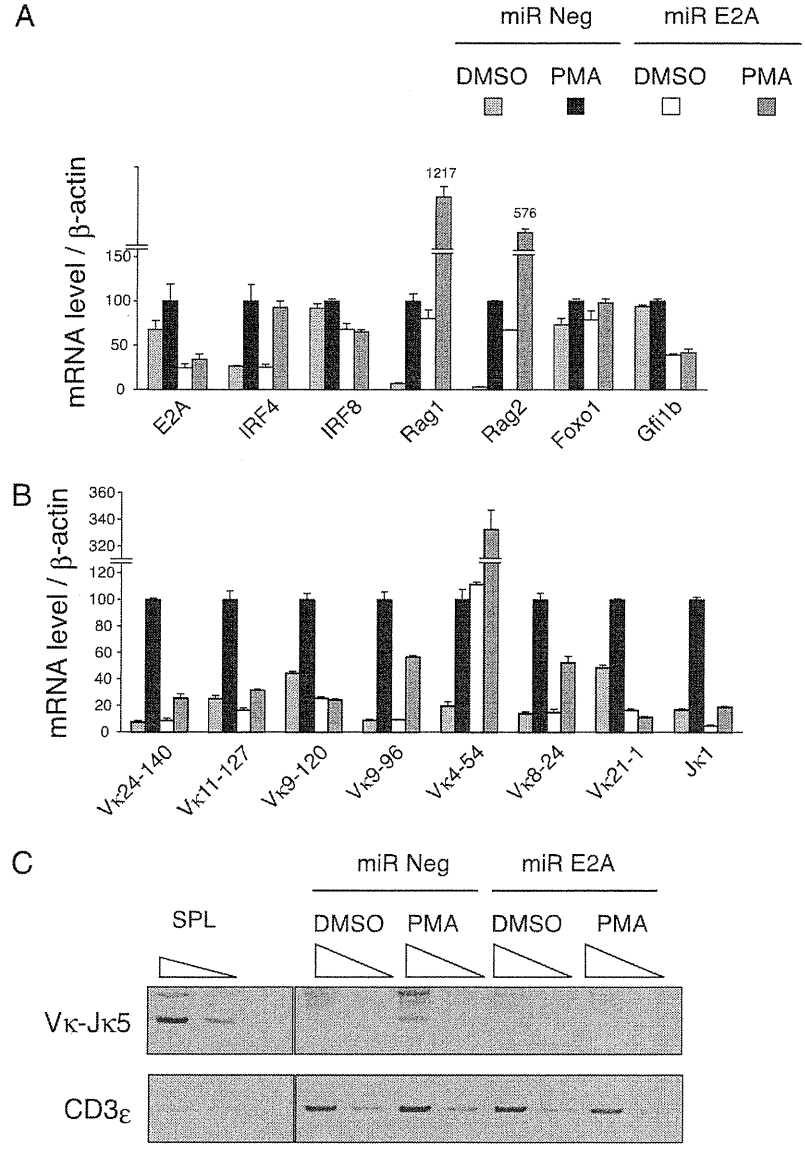

FIGURE 9. Knockdown of E2A expression reduces PMA-induced Vκ and Jκ GLTs and Vκ-Jκ rearrangement. (**A**) RT-PCR analysis of the genes involved in *Igκ* rearrangement. RNA was isolated from BKO84 cells transduced with retrovirus expressing negative control miRNA or E2A-specific miRNA in the absence (DMSO) or presence of PMA and analyzed for the expression of indicated genes by real-time RT-PCR. Expression levels were normalized to β-actin mRNA levels. Relative mRNA levels are shown as the mean of triplicate PCRs with SD, and the levels in BKO84 cells expressing negative control miRNA in the presence of PMA are set to 100 for each transcript. Data are representative of three independent experiments. (**B**) RT-PCR analysis of Vκ and Jκ GLT. RT-PCR was performed as in (A). (**C**) Genomic PCR analysis of Vκ-Jκ rearrangement. Genomic DNA was isolated from BKO84 cells transduced as in (A) and analyzed for Vκ-Jκ rearrangement by semiquantitative PCR (60 and 15 ng). Genomic DNA was also isolated from splenocytes and used as a positive control (5 and 1.25 ng). The mouse CD3ε gene was also analyzed as a loading control. Data are representative of three independent experiments.

cells, supporting the notion that the critical function of E2A to induce recombination might be to induce the local accessibility of rearranging gene segments by recruiting HAT complexes rather than to induce transcription itself. Furthermore, the observation that E2A directly binds to the promoter and RSS regions of the VκI gene family members may explain how E2A could induce localized gene-specific accessibility, which was reported previously (43).

Knockdown of CBP/p300 in BOSC23 cells markedly diminished the E2A-induced acetylation of H3K9 and H3K18 at both the VκI promoter and RSS regions, whereas overexpression of CBP/p300 enhanced only H3K18ac, but not H3K9ac. One possible explanation for this discrepancy is that both H3K9ac and H3K18ac are catalyzed by CBP/p300, but that the threshold for the amount of CBP/p300 required for the acetylation reaction is different between H3K9 and H3K18. For H3K9ac, a lower amount of endogenous CBP/p300 recruited by the limited amount of E2A proteins upon coexpression might be sufficient, and overexpressed CBP/p300 could not contribute to further enhancement of acetylation (Fig. 2). In contrast, endogenous CBP/p300 recruited by E2A alone may not be sufficient for H3K18ac, which is increased only after overexpression of CBP/p300 (Fig. 2). Another possibility is that H3K9ac might be catalyzed by a HAT other than CBP/p300, whereas H3K18ac might be catalyzed directly by CBP/p300. However, H3K9ac may be dependent on H3K18ac. Furthermore, this discrepancy might be consistent with the recent study demonstrating that p300/CBP-dependent H3K18ac is required for transcriptional induction by adenovirus e1a, whereas changes in H3K9ac are not sufficient for transcriptional induction (44).

We further analyzed a mouse pre-B cell line, BKO84, derived from a BLNK-deficient mouse and confirmed that endogenous E2A proteins also have the ability to bind some Vκ genes in a more physiological situation. In the absence of PMA, considerable levels of E2A binding were detected at the distinct set of Vκ genes albeit at lower levels than those at iEκ and 3′Eκ. PMA treatment increased the E2A binding level at the corresponding Vκ genes as well as at iEκ and 3′Eκ, accompanied by a concomitant increase in E2A mRNA and protein expression. A recent study reported that activation of the Ras–MEK–ERK pathway is essential for maintaining E2A expression and downregulating Id3, thereby contributing to the high net free E2A level (45). Consistent with this finding, PMA treatment of BKO84 cells led to activation of ERK (25), suggesting that activation of ERK might contribute to the increased E2A binding. E2A knockdown resulted in a sub-

stantial reduction of the E2A binding levels at most of the regions in the *Igκ* locus, accompanied by concomitant decreases in p300 recruitment and histone acetylation at Vκ genes, GLTs of Vκ and Jκ genes, and Vκ-Jκ rearrangement.

It is noteworthy that E2A binds to distinct Vκ genes at variable levels from highest levels at Vκ11-127, Vκ9-120, and Vκ9-96 among those examined to a marginal level at Vκ4-54. Notably, Vκ11-127, Vκ9-120, and Vκ9-96 genes are reported to be members of the mouse Vκ family homologous to the human VκI gene family (12, 46). This is consistent with the finding that overexpressed E2A can induce rearrangement specifically involving the VκI gene family members in BOSC23 cells (8, 43). Thus, it is intriguing to speculate that E2A might be involved in Vκ repertoire selection by direct binding to the distinct set of Vκ genes in an evolutionally conserved manner. Genome-wide analysis including ChIP sequencing is necessary to clarify this issue. Consistent with the observation that E2A binding was marginal at Vκ4-54, the Vκ4-54 gene does not have any putative E-box sites around the gene, whereas other Vκ genes that show considerable E2A binding contain at least one E-box site around the gene (13). Moreover, E2A knockdown did not lead to a decrease, but rather an increase in both the H3K18ac and GLT levels of the Vκ4-54 gene, suggesting that Vκ4-54 is regulated by other factors than E2A and such factors may compete for HATs with E2A. In support of this hypothesis, it was reported that the binding sites for EBF, but not E2A, are conserved in the introns of a group of Vκ4 genes (13). With regard to the competition for HATs, however, we could not observe an apparent increase in the recruitment of p300 at Vκ4-54 upon E2A knockdown presumably due to the detection limits of the p300 ChIP (data not shown). Alternatively, in addition to the accessibility control, E2A would also be involved in locus contraction as reported for YY1 in the *IgH* locus, as E2A can bind to both the distinct set of Vκ genes and the enhancers as shown for YY1 in the *IgH* locus (47).

The previous studies have demonstrated the functional importance of iEκ and 3′Eκ enhancers in *Igκ* rearrangement during B cell development in vivo (6, 16, 38). Targeted mutation of the E2A-binding motifs in iEκ impairs *Igκ* rearrangement (16), directly demonstrating the crucial functions of E2A and iEκ in *Igκ* rearrangement in vivo. It was shown that IRF4 functions to facilitate the association of E2A to 3′Eκ and that E2A acts in synergy with IRF4 to increase histone acetylation at 3′Eκ and Jκ GLT, thereby promoting *Igκ* rearrangement (39). Notably, IRF4/8 double-knockout pre-B cells fail to activate Ig L chain recombination; however, IL-7 withdrawal from the culture leads to the increased histone acetylation and E2A occupancy at iEκ and induction of *Igκ* gene recombination (35, 45). Consistent with these findings, it was recently reported that IL-7 signaling inhibits *Igκ* recombination by forming a STAT5 tetramer bound to iEκ, which antagonizes E2A for binding (48). Because iEκ, but not 3′Eκ, is required for accessibility of the Vκ genes (38) and also the Jκ region (49), lowering of IL-7 signaling might promote *Igκ* recombination by inducing the accessibility of the Vκ genes and the Jκ region via activation of iEκ, which involves E2A recruitment.

The findings described above have clearly demonstrated that a critical function of E2A in increasing the accessibility of the *Igκ* locus is the activation of the iEκ and 3′Eκ enhancers through direct binding and increasing histone acetylation. Thus, it was surprising that E2A overexpression in BOSC23 cells did not efficiently increase histone acetylation at these κ enhancers despite the fact that E2A expression induced Jκ GLT in this cell line. However, we reproducibly observed that E2A bound more efficiently to iEκ than to 3′Eκ in BOSC23 cells, albeit at lower levels compared with the Vκ genes (Fig. 1B). This might be consistent with the finding that iEκ, but not 3′Eκ, is essential for the Vκ gene accessibility, which was indeed increased upon E2A expression (38). As described earlier, IRF4 is required for the activation of 3′Eκ by facilitating the E2A recruitment and histone acetylation at 3′Eκ, but we found that IRF4 is not expressed in BOSC23 cells (data not shown). Thus, we overexpressed IRF4 together with E2A in BOSC23 cells, but we did not observe any synergistic effect on the frequency of *Igκ* recombination. This might be because additional factors including PU.1 are required for the interaction of IRF4 with 3′Eκ in BOSC23 cells; however, addition of PU.1 did not facilitate *Igκ* recombination. Alternatively, it might be because B cell-specific modifications of the IRF4 and PU.1 proteins such as phosphorylation are required for the synergistic function with E2A (50). Further genome-wide analyses including ChIP sequencing and chromosome conformation capture assay for *cis*-acting elements and transcription factors including E2A will be necessary to elucidate the molecular processes of Vκ repertoire formation and locus contraction at the chromosome level.

Acknowledgments

We thank Drs. S.W. Lowe and A. Yu for MSCV-PIG dRI, T. Kitamura for Plat-E cells, Y. Zhuang, B. Jones, and A. Lazorchak for E2A knockout pre-B lines, M. Atchison for expression plasmids, and H. Kimura, K. Tanigaki, and the staff of Horizontal Medical Research Organization, the Murre laboratory, and the Minato laboratory for discussions and materials. We thank S. Tanaka for technical assistance.

Disclosures

The authors have no financial conflicts of interest.

References

1. Bassing, C. H., W. Swat, and F. W. Alt. 2002. The mechanism and regulation of chromosomal V(D)J recombination. *Cell* 109(Suppl): S45–S55.
2. Jung, D., and F. W. Alt. 2004. Unraveling V(D)J recombination; insights into gene regulation. *Cell* 116: 299–311.
3. Krangel, M. S. 2003. Gene segment selection in V(D)J recombination: accessibility and beyond. *Nat. Immunol.* 4: 624–630.
4. Sleckman, B. P., J. R. Gorman, and F. W. Alt. 1996. Accessibility control of antigen-receptor variable-region gene assembly: role of cis-acting elements. *Annu. Rev. Immunol.* 14: 459–481.
5. Schlissel, M. S. 2004. Regulation of activation and recombination of the murine Igkappa locus. *Immunol. Rev.* 200: 215–223.
6. Inlay, M., F. W. Alt, D. Baltimore, and Y. Xu. 2002. Essential roles of the kappa light chain intronic enhancer and 3′ enhancer in kappa rearrangement and demethylation. *Nat. Immunol.* 3: 463–468.
7. Murre, C. 2005. Helix-loop-helix proteins and lymphocyte development. *Nat. Immunol.* 6: 1079–1086.
8. Romanow, W. J., A. W. Langerak, P. Goebel, I. L. Wolvers-Tettero, J. J. van Dongen, A. J. Feeney, and C. Murre. 2000. E2A and EBF act in synergy with the V(D)J recombinase to generate a diverse immunoglobulin repertoire in nonlymphoid cells. *Mol. Cell* 5: 343–353.
9. Murre, C., P. S. McCaw, and D. Baltimore. 1989. A new DNA binding and dimerization motif in immunoglobulin enhancer binding, daughterless, MyoD, and myc proteins. *Cell* 56: 777–783.
10. Pongubala, J. M., and M. L. Atchison. 1991. Functional characterization of the developmentally controlled immunoglobulin kappa 3′ enhancer: regulation by Id, a repressor of helix-loop-helix transcription factors. *Mol. Cell. Biol.* 11: 1040–1047.
11. Greenbaum, S., and Y. Zhuang. 2002. Identification of E2A target genes in B lymphocyte development by using a gene tagging-based chromatin immunoprecipitation system. *Proc. Natl. Acad. Sci. USA* 99: 15030–15035.
12. Bemark, M., D. Liberg, and T. Leanderson. 1998. Conserved sequence elements in K promoters from mice and humans: implications for transcriptional regulation and repertoire expression. *Immunogenetics* 47: 183–195.
13. Brekke, K. M., and W. T. Garrard. 2004. Assembly and analysis of the mouse immunoglobulin kappa gene sequence. *Immunogenetics* 56: 490–505.
14. Feeney, A. J., G. Lugo, and G. Escuro. 1997. Human cord blood kappa repertoire. *J. Immunol.* 158: 3761–3768.
15. Schäble, K. F., and H. G. Zachau. 1993. The variable genes of the human immunoglobulin kappa locus. *Biol. Chem. Hoppe Seyler* 374: 1001–1022.
16. Inlay, M. A., H. Tian, T. Lin, and Y. Xu. 2004. Important roles for E protein binding sites within the immunoglobulin kappa chain intronic enhancer in activating Vkappa Jkappa rearrangement. *J. Exp. Med.* 200: 1205–1211.
17. Ghosh, J. K., W. J. Romanow, and C. Murre. 2001. Induction of a diverse T cell receptor gamma/delta repertoire by the helix-loop-helix proteins E2A and HEB in nonlymphoid cells. *J. Exp. Med.* 193: 769–776.

18. Bradney, C., M. Hjelmeland, Y. Komatsu, M. Yoshida, T. P. Yao, and Y. Zhuang. 2003. Regulation of E2A activities by histone acetyltransferases in B lymphocyte development. *J. Biol. Chem.* 278: 2370–2376.
19. Eckner, R., T. P. Yao, E. Oldread, and D. M. Livingston. 1996. Interaction and functional collaboration of p300/CBP and bHLH proteins in muscle and B-cell differentiation. *Genes Dev.* 10: 2478–2490.
20. Massari, M. E., P. A. Grant, M. G. Pray-Grant, S. L. Berger, J. L. Workman, and C. Murre. 1999. A conserved motif present in a class of helix-loop-helix proteins activates transcription by direct recruitment of the SAGA complex. *Mol. Cell* 4: 63–73.
21. Qiu, Y., A. Sharma, and R. Stein. 1998. p300 mediates transcriptional stimulation by the basic helix-loop-helix activators of the insulin gene. *Mol. Cell. Biol.* 18: 2957–2964.
22. Sayegh, C. E., M. W. Quong, Y. Agata, and C. Murre. 2003. E-proteins directly regulate expression of activation-induced deaminase in mature B cells. *Nat. Immunol.* 4: 586–593.
23. Chrivia, J. C., R. P. Kwok, N. Lamb, M. Hagiwara, M. R. Montminy, and R. H. Goodman. 1993. Phosphorylated CREB binds specifically to the nuclear protein CBP. *Nature* 365: 855–859.
24. Eckner, R., M. E. Ewen, D. Newsome, M. Gerdes, J. A. DeCaprio, J. B. Lawrence, and D. M. Livingston. 1994. Molecular cloning and functional analysis of the adenovirus E1A-associated 300-kD protein (p300) reveals a protein with properties of a transcriptional adaptor. *Genes Dev.* 8: 869–884.
25. Yamamoto, M., K. Hayashi, T. Nojima, Y. Matsuzaki, Y. Kawano, H. Karasuyama, R. Goitsuka, and D. Kitamura. 2006. BASH-novel PKC-Raf-1 pathway of pre-BCR signaling induces kappa gene rearrangement. *Blood* 108: 2703–2711.
26. Dickins, R. A., M. T. Hemann, J. T. Zilfou, D. R. Simpson, I. Ibarra, G. J. Hannon, and S. W. Lowe. 2005. Probing tumor phenotypes using stable and regulated synthetic microRNA precursors. *Nat. Genet.* 37: 1289–1295.
27. Morita, S., T. Kojima, and T. Kitamura. 2000. Plat-E: an efficient and stable system for transient packaging of retroviruses. *Gene Ther.* 7: 1063–1066.
28. Agata, Y., T. Katakai, S. K. Ye, M. Sugai, H. Gonda, T. Honjo, K. Ikuta, and A. Shimizu. 2001. Histone acetylation determines the developmentally regulated accessibility for T cell receptor gamma gene recombination. *J. Exp. Med.* 193: 873–880.
29. Agata, Y., N. Tamaki, S. Sakamoto, T. Ikawa, K. Masuda, H. Kawamoto, and C. Murre. 2007. Regulation of T cell receptor beta gene rearrangements and allelic exclusion by the helix-loop-helix protein, E47. *Immunity* 27: 871–884.
30. Engel, I., C. Johns, G. Bain, R. R. Rivera, and C. Murre. 2001. Early thymocyte development is regulated by modulation of E2A protein activity. *J. Exp. Med.* 194: 733–745.
31. Schiltz, R. L., C. A. Mizzen, A. Vassilev, R. G. Cook, C. D. Allis, and Y. Nakatani. 1999. Overlapping but distinct patterns of histone acetylation by the human coactivators p300 and PCAF within nucleosomal substrates. *J. Biol. Chem.* 274: 1189–1192.
32. Daujat, S., U. M. Bauer, V. Shah, B. Turner, S. Berger, and T. Kouzarides. 2002. Crosstalk between CARM1 methylation and CBP acetylation on histone H3. *Curr. Biol.* 12: 2090–2097.
33. Horwitz, G. A., K. Zhang, M. A. McBrian, M. Grunstein, S. K. Kurdistani, and A. J. Berk. 2008. Adenovirus small e1a alters global patterns of histone modification. *Science* 321: 1084–1085.
34. Schlissel, M., A. Constantinescu, T. Morrow, M. Baxter, and A. Peng. 1993. Double-strand signal sequence breaks in V(D)J recombination are blunt, 5′-phosphorylated, RAG-dependent, and cell cycle regulated. *Genes Dev.* 7(12B): 2520–2532.
35. Johnson, K., T. Hashimshony, C. M. Sawai, J. M. Pongubala, J. A. Skok, I. Aifantis, and H. Singh. 2008. Regulation of immunoglobulin light-chain recombination by the transcription factor IRF-4 and the attenuation of interleukin-7 signaling. *Immunity* 28: 335–345.
36. Lu, R., K. L. Medina, D. W. Lancki, and H. Singh. 2003. IRF-4,8 orchestrate the pre-B-to-B transition in lymphocyte development. *Genes Dev.* 17: 1703–1708.
37. Oda, A., T. Ono, M. Yamamoto, R. Goitsuka, and D. Kitamura. 2008. PKC eta directs induction of IRF-4 expression and Ig kappa gene rearrangement in pre-BCR signaling pathway. *Int. Immunol.* 20: 1417–1426.
38. Inlay, M. A., T. Lin, H. H. Gao, and Y. Xu. 2006. Critical roles of the immunoglobulin intronic enhancers in maintaining the sequential rearrangement of IgH and Igk loci. *J. Exp. Med.* 203: 1721–1732.
39. Lazorchak, A. S., M. S. Schlissel, and Y. Zhuang. 2006. E2A and IRF-4/Pip promote chromatin modification and transcription of the immunoglobulin kappa locus in pre-B cells. *Mol. Cell. Biol.* 26: 810–821.
40. Schulz, D., L. Vassen, K. T. Chow, S. M. McWhirter, R. H. Amin, T. Möröy, and M. S. Schlissel. 2012. Gfi1b negatively regulates Rag expression directly and via the repression of FoxO1. *J. Exp. Med.* 209: 187–199.
41. Schwartz, R., I. Engel, M. Fallahi-Sichani, H. T. Petrie, and C. Murre. 2006. Gene expression patterns define novel roles for E47 in cell cycle progression, cytokine-mediated signaling, and T lineage development. *Proc. Natl. Acad. Sci. USA* 103: 9976–9981.
42. Xu, W., and B. L. Kee. 2007. Growth factor independent 1B (Gfi1b) is an E2A target gene that modulates Gata3 in T-cell lymphomas. *Blood* 109: 4406–4414.
43. Goebel, P., N. Janney, J. R. Valenzuela, W. J. Romanow, C. Murre, and A. J. Feeney. 2001. Localized gene-specific induction of accessibility to V(D)J recombination induced by E2A and early B cell factor in nonlymphoid cells. *J. Exp. Med.* 194: 645–656.
44. Ferrari, R., M. Pellegrini, G. A. Horwitz, W. Xie, A. J. Berk, and S. K. Kurdistani. 2008. Epigenetic reprogramming by adenovirus e1a. *Science* 321: 1086–1088.
45. Mandal, M., S. E. Powers, K. Ochiai, K. Georgopoulos, B. L. Kee, H. Singh, and M. R. Clark. 2009. Ras orchestrates exit from the cell cycle and light-chain recombination during early B cell development. *Nat. Immunol.* 10: 1110–1117.
46. Kroemer, G., A. Helmberg, A. Bernot, C. Auffray, and R. Kofler. 1991. Evolutionary relationship between human and mouse immunoglobulin kappa light chain variable region genes. *Immunogenetics* 33: 42–49.
47. Guo, C., T. Gerasimova, H. Hao, I. Ivanova, T. Chakraborty, R. Selimyan, E. M. Oltz, and R. Sen. 2011. Two forms of loops generate the chromatin conformation of the immunoglobulin heavy-chain gene locus. *Cell* 147: 332–343.
48. Mandal, M., S. E. Powers, M. Maienschein-Cline, E. T. Bartom, K. M. Hamel, B. L. Kee, A. R. Dinner, and M. R. Clark. 2011. Epigenetic repression of the Igk locus by STAT5-mediated recruitment of the histone methyltransferase Ezh2. *Nat. Immunol.* 12: 1212–1220.
49. Xu, C. R., and A. J. Feeney. 2009. The epigenetic profile of Ig genes is dynamically regulated during B cell differentiation and is modulated by pre-B cell receptor signaling. *J. Immunol.* 182: 1362–1369.
50. Pongubala, J. M., C. Van Beveren, S. Nagulapalli, M. J. Klemsz, S. R. McKercher, R. A. Maki, and M. L. Atchison. 1993. Effect of PU.1 phosphorylation on interaction with NF-EM5 and transcriptional activation. *Science* 259: 1622–1625.

A Vκ RSS H3K9/14ac ChIP

Vκ genes	Clone number
O2/O12	7
L18	7
L11	4
A4	4
L19	3
L12a	3
L8	3
A20	3
A30	3
Chr 9 V108	3
L23	2
L9	1
L1	1
Total number	44

B VκI GLT

Vκ genes	Clone number
L19	16
O2/O12	6
L11	6
L9	6
L18	3
Chr 9 V108	3
A4	2
L23	2
A30	1
L12a	1
L1	1
Chr 22 pseudo	1
pseudo w3	1
Total number	49

Supplemental Table 1. Vκ gene segments analyzed in VκI RSS H3K9/14ac ChIP and VκI GLT samples are diverse.

(A) VκI RSS fragments amplified by PCR from H3K9/14ac ChIP samples of E2A-transfected BOSC23 cells were cloned and sequenced. Vκ gene segments and the numbers of isolated clones are indicated. Note that O2/O12, L11, L12a, L8, A20, A30, and L9 were also found in 10 Vκ gene segments that were identified for VκI-Jκ gene rearrangements in E2A-transfected BOSC23 cells (Romanow et al. Mol. Cell 5: 343, 2000). (B) E2A-induced VκI GLTs amplified by RT-PCR were cloned and sequenced. Vκ gene segments and the numbers of isolated clones are indicated.

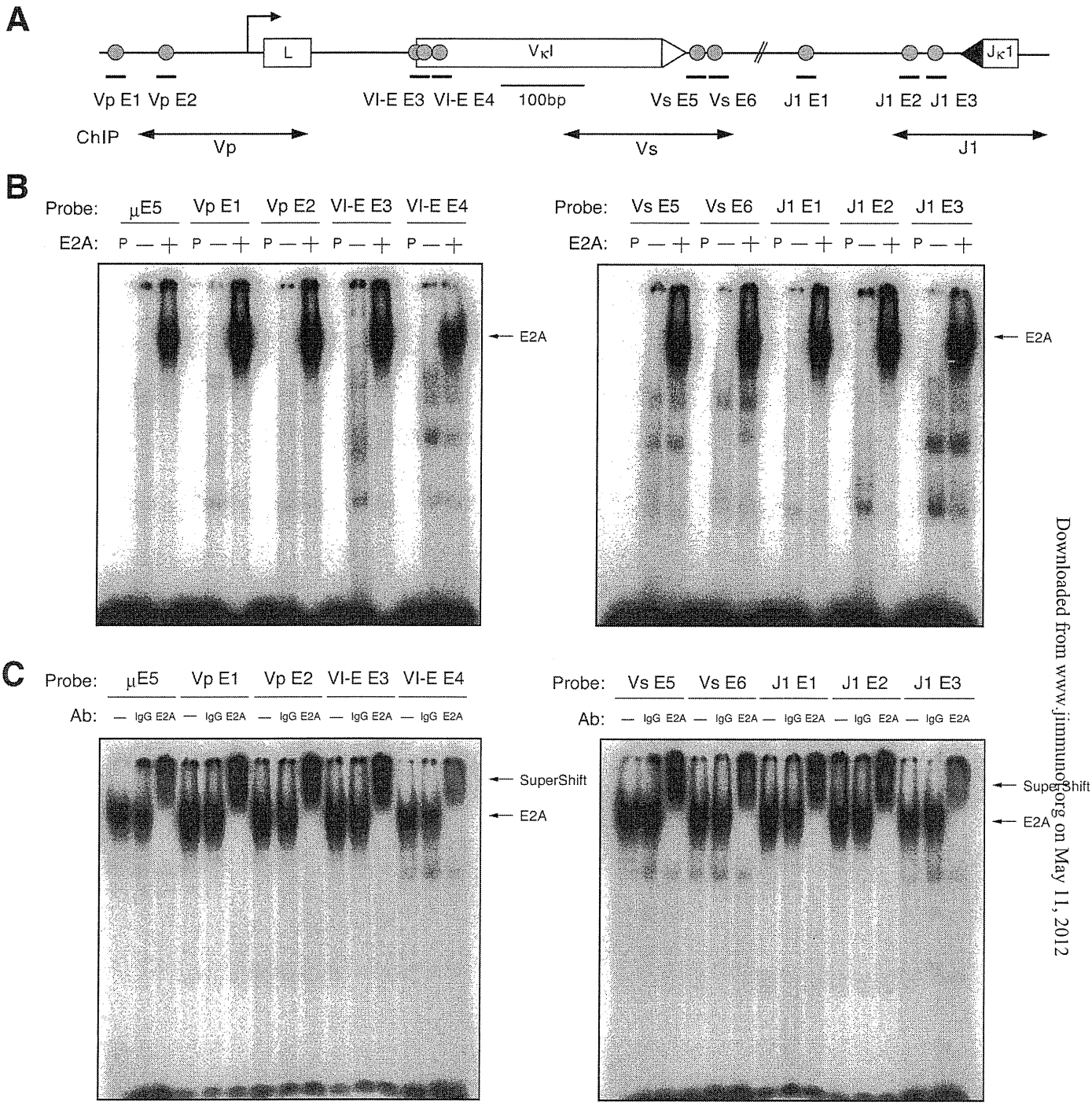

Supplemental Figure 1. E2A binds to E-box sites around human Vκl and Jκ1gene segments in vitro.

(A) Schematic illustration of the human Vκl and Jκ1gene segments and location of E-box sites (gray circles), EMSA probes (bars below the E-box sites) and the PCR-amplified regions analyzed in ChIP-qPCR (arrows). The leader (L) and Vκl, Jκ1 exons are indicated by boxes. The Vκl RSS with a 12-bp spacer and Jκ1 RSS with a 23-bp spacer are indicated by open and filled triangles, respectively. (B) EMSA analysis of E2A DNA-binding activity in transfected BOSC23 cells. Nuclear extracts were prepared from BOSC23 cells transfected with mock (-) or E2A (+) plasmid, and analyzed for the binding activity to the μE5 probe (control) or probes containing E-box sites around Vκl and Jκ1gene segments. Free probes were run in parallel (P). The position of the shifted binding complex is indicated (E2A). (C) The specificity of E2A DNA-binding complex was examined using control normal rabbit IgG (IgG) or an anti-E2A antibody (E2A). The specific binding complexes (E2A) and supershifted complexes are indicated.

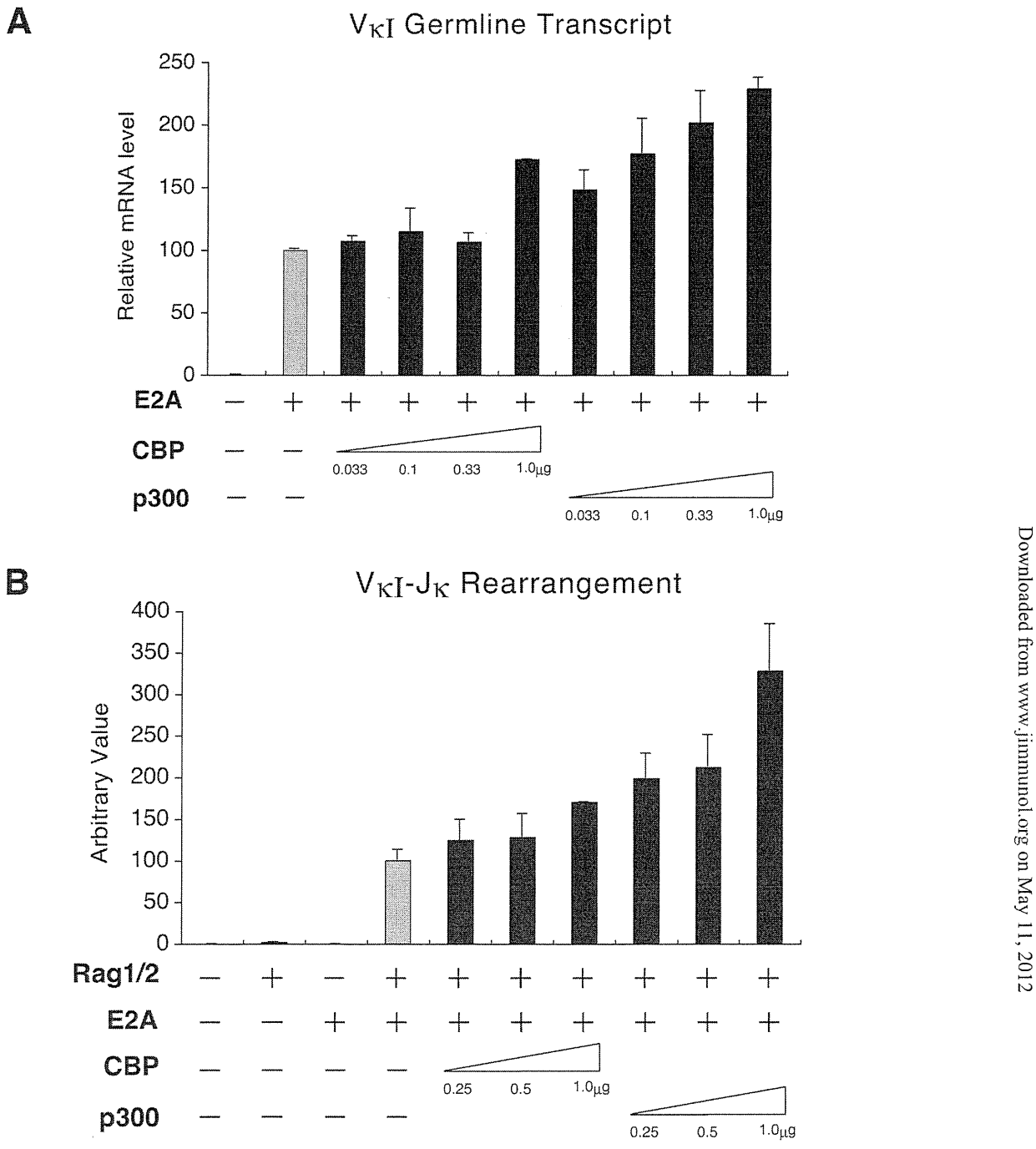

Supplemental Figure 2. Increasing amounts of CBP/p300 expression vectors lead to the graded responses in E2A-induced VκI GLT and VκI-Jκ rearrangement

(A) RT-PCR analysis of VκI GLT. RNA was isolated from BOSC23 cells transfected with indicated amounts of expression plasmids (for E2A +, 0.67μg was used) and analyzed for VκI GLT by real-time RT-PCR. VκI GLT levels were normalized to β -actin mRNA levels, and relative mRNA levels are shown as the mean of triplicate PCRs with SD. Data are representative of two independent experiments. (B) Genomic PCR analysis of VκI-Jκ rearrangement. Genomic DNA was isolated from BOSC23 cells transfected with indicated amounts of expression plasmids (for E2A, Rag1 or Rag2 +, 0.67μg was used) and analyzed for VκI-Jκ rearrangement by real-time PCR. VκI-Jκ rearrangement levels were normalized to the CD14 gene, and normalized rearrangement levels in arbitrary values are shown as the mean of triplicate PCRs with SD. Data are representative of two independent experiments.

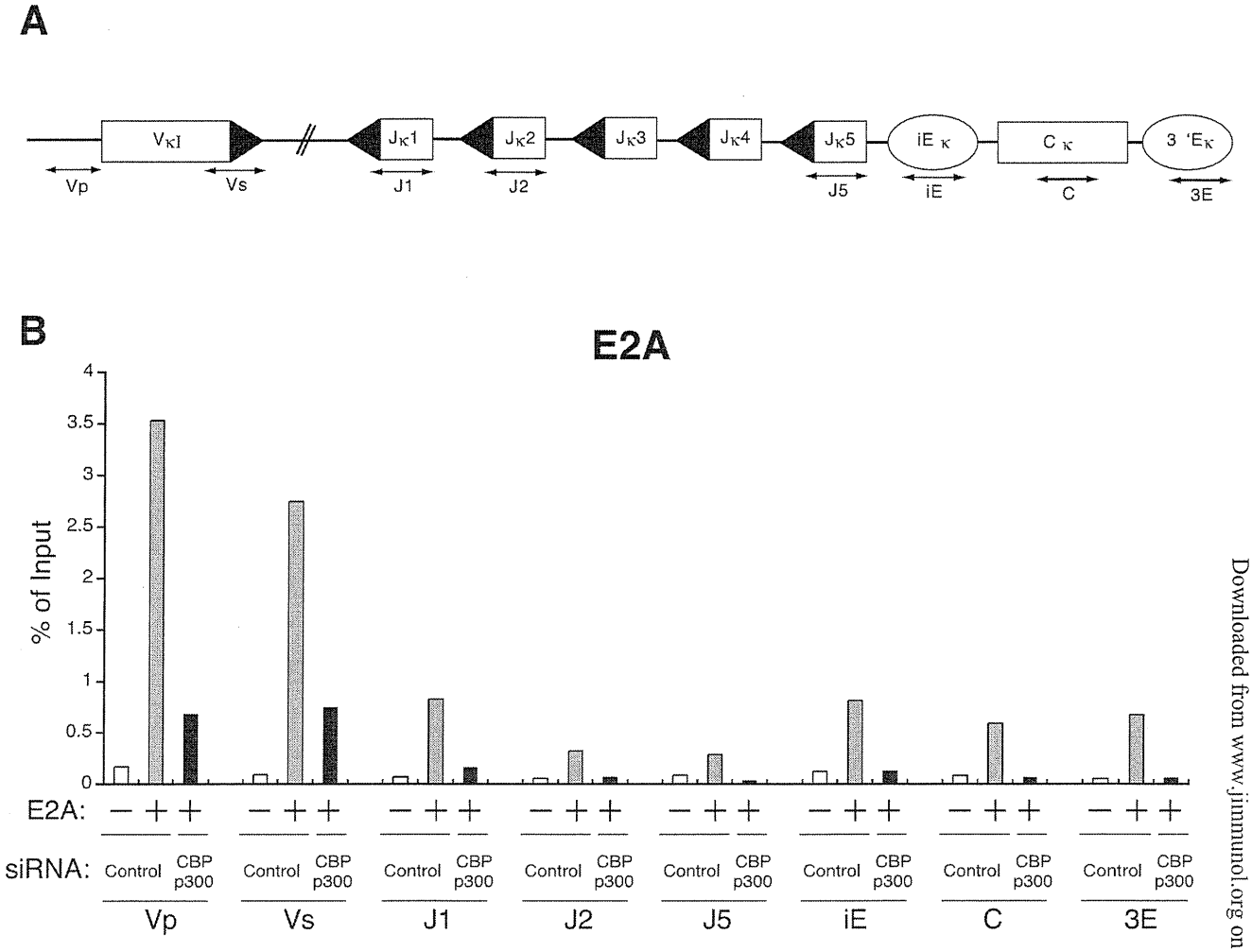

Supplemental Figure 3. Knockdown of CBP/p300 reduces E2A occupancy throughout the Igκ locus.

(A) A schematic diagram of the human Igκ locus. Boxes, triangles, and ellipses represent gene segments, RSSs, and enhancer regions, respectively. Locations of the amplified regions in ChIP analysis are shown below, Vκ1 promoter (Vp), Vκ1 RSS (Vs), Jκ1, Jκ2, Jκ5 gene segment (J1, J2, J5), iEκ (iE), constant region gene (C) and 3' Eκ (3E). (B) ChIP analysis of E2A binding throughout the Igκ locus in BOSC23 cells transfected with mock plasmid and negative control siRNA (white bar), E2A and negative control siRNA (gray bar), E2A and CBP/p300-specific siRNA (black bar). Chromatin was prepared from transfected BOSC23 cells enriched for CD25 coexpression marker and immunoprecipitated with antibodies against E2A. The bound and input fractions were quantified by real-time PCR, and ratios of bound/input are indicated as a percentage of input for each region.